Hindawi
Advances in Materials Science and Engineering
Volume 2024, Article ID 6262251, 29 pages
https://doi.org/10.1155/2024/6262251

Research Article

Water Absorption, Thermal, and Mechanical Properties of Bamboo Fiber with Chopped Glass Fiber Filler-Reinforced Polyester Composites

Mohammed Abdulkedir Alfeki and Ephrem Assefa Feyissa

Department of Mechanical Engineering, College of Engineering and Technology, Bule Hora University, P.O. Box 144, Bule Hora, Ethiopia

Correspondence should be addressed to Mohammed Abdulkedir Alfeki; mohammed@bhu.edu.et

Received 13 November 2023; Revised 28 February 2024; Accepted 4 April 2024; Published 30 April 2024

Academic Editor: Hafsa Jamshaid

This study explores the investigations of bamboo fiber-reinforced polyester composites with chopped glass fiber (CGF) filler, focusing on addressing the challenges of low mechanical properties, limited thermal stability, and high moisture absorption. The two types of composites were fabricated using the hand layup method, that is, long unidirectional 0° bamboo fiber (BF) and randomly oriented short bamboo fiber (BP) reinforced a polyester matrix with chopped glass fiber (CGF) filler. By incorporating CGF filler, significant improvements in mechanical properties were achieved across both types of bamboo fiber, surpassing the limitations of unfilled composites. Notably, the composite formulation consisting of 40% wt. of unidirectional 0° BF and 5% wt. of CGF filler exhibited superior ultimate tensile strength, flexural strength, impact strength, water absorption, and thermal stability. This composite demonstrated remarkable enhancements, with increases of up to 131.22 MPa, 128.76 MPa, 113.3 kJ/m^2, 1.94% water absorption, and up to 255°C (representing a 10% improvement) in thermal stability compared to the unfilled composite. Statistical analysis revealed quadratic models for the mechanical properties of long unidirectional 0° bamboo fiber composites, while water absorption exhibited a linear two-factor interaction model. For randomly oriented short bamboo fiber, the models for tensile, flexural, and water absorption properties were linear, while the impact energy model showed a quadratic relationship. These statistical models provide valuable insights into predicting the properties of bamboo fiber-reinforced polyester composites. This research underscores the significance of bamboo fiber-reinforced polyester composites in wall partition systems. This study paves the way for improved performance in these areas. The findings highlight the potential of incorporating CGF filler, enabling enhanced mechanical strength, increased thermal stability, and improved resistance to moisture-related issues. The derived statistical models offer valuable guidance for predicting the properties of these composites, facilitating their application and adoption in the construction industry.

1. Introduction

In recent years, composite materials have emerged as a focal point of research and development due to their ability to enhance mechanical and physical properties by combining different materials [1]. Among these materials, natural fiber composites have gained considerable attention for their renewable and biodegradable characteristics [2]. In Ethiopia, the exploration of natural fibers, particularly bamboo, has witnessed significant growth, with highland bamboo species being extensively studied for their dense fibers and ease of extraction compared to lowland bamboo [3].

However, bamboo fiber composites face challenges in achieving optimal mechanical and physical properties [4–6]. These composites often exhibit drawbacks such as higher moisture absorption, inferior fire resistance, lower mechanical properties, and poor adhesion to the polymeric matrix, which are critical factors in applications such as wall partition systems [3, 7]. To overcome these limitations, one approach involves the incorporation of filler materials, particularly synthetic fillers known for their hydrophobic properties [5, 6, 8, 9]. However, the cost associated with synthetic fillers remains a concern, necessitating the search for alternative cost-effective solutions [10]. Additionally, understanding the influence of fiber weight on composite properties is crucial for optimizing their performance in specific applications, such as wall partitions [11].

Wall partition systems play a crucial role in modern construction, providing functional and aesthetic separations within buildings [12, 13] and marines [14]. However, conventional partition materials often face challenges such as low mechanical properties, limited thermal stability, and high moisture absorption, which can compromise the integrity and longevity of the partitions [15, 16]. Addressing these challenges requires the development of advanced composite materials that exhibit enhanced performance in these key areas.

In this context, the utilization of waste-chopped glass fibers, a commonly available synthetic fiber with significant wastage during composite manufacturing and other processes, becomes crucial for enhancing the physical and mechanical properties of bamboo fiber-reinforced polyester composites for wall partition systems in a cost-effective manner [17]. Polyester, chosen as the matrix material, offers several advantages, including its lightweight nature, good electrical insulation, corrosion and weathering resistance, abrasion resistance, and cost-effectiveness [18]. Previous studies have demonstrated that the incorporation of fibers and particulates, such as chopped glass fiber, can significantly enhance the mechanical properties of polyester composites [19].

While previous research has investigated various parameters, such as fiber weight, length, and chemical treatments, on the properties of bamboo composites, the specific impact of varying the weights of chopped glass fiber and bamboo fiber remains relatively unexplored [20–24]. Other limitations of previous studies are that only one set of samples was tested for each type of composite, and the statistical significance of the results may not be fully realized [25]. This research gap necessitates an in-depth investigation into the water absorption, thermal stability, and mechanical properties of bamboo fiber with chopped glass fiber filler-reinforced polyester composites, with a specific focus on the weight ratios of these components, particularly for their application in wall partition systems.

This study aims to comprehensively investigate the water absorption, thermal stability, and mechanical properties of bamboo fiber with chopped glass fiber filler-reinforced polyester composites for wall partition systems, with a particular emphasis on varying the weights of chopped glass fiber and bamboo fiber. By examining these parameters, the research aims to gain valuable insights into how the weight ratios of these components influence the characteristics of the composite material, specifically when utilized in wall partition applications.

Understanding the water absorption properties of the composite is crucial for wall partition systems, where moisture resistance is essential to maintain structural integrity and prevent degradation [26]. Likewise, investigating the thermal properties is vital to assessing the composite's performance under different temperature conditions, ensuring its suitability for wall partitions in various environments [27]. Finally, the mechanical properties, including tensile strength, flexural strength, and impact resistance, are of utmost importance in evaluating the composite's structural integrity and longevity in wall partition systems [28].

This investigation holds significant importance as it contributes to the growing body of knowledge on natural fiber composites and provides valuable insights into the potential applications of bamboo fiber composites in wall partition systems within the construction industry [29–33]. Moreover, by exploring the influence of chopped glass fiber weight and bamboo fiber weight on the composite's properties, this research aims to optimize the formulation of these composites, leading to improved performance, durability, and cost-effectiveness in wall partition applications.

2. Materials and Methods

To achieve the objectives of this study, the following activities were conducted:

Fabrication of the specimen sample: The fabrication process involved creating composite specimens with different weight percentages. These weight percentages were determined based on a combination of trials generated using the Central Composite Design (CCD) method, which is a response surface methodology (RSM). The specimens were fabricated using long unidirectional 0° bamboo fibers and randomly oriented short bamboo fibers, along with a filler material consisting of waste or collected chopped glass fibers (CGF). The bamboo fiber and CGF were reinforced with a polyester matrix.

Determination of mechanical and physical properties: The fabricated specimens were subjected to mechanical testing to determine their tensile, flexural, and impact properties. Additionally, the physical properties, such as water absorption and thermal stability, or thermogravimetric analysis (TGA), were evaluated. These tests provided valuable insights into the structural integrity, strength, and durability of the composite material.

Evaluation of the effect of long bamboo fiber (BF), short bamboo fiber (BP), and CGF weight percentages: The weight percentages of bamboo fiber to polyester (BF/BP) and CGF were varied in the fabrication process. The aim was to investigate the influence of these weight percentages on the mechanical and physical properties of the composite material. By analyzing the data, the relationship between the weight percentages and the properties of the composite could be established.

Statistical analysis: Statistical analysis was performed to analyze the mechanical and physical properties of the composite material. This analysis involved techniques such as regression analysis and analysis of variance (ANOVA), which helped determine the significance of the factors and their interactions. The statistical analysis provided quantitative insights into the relationship between the weight percentages and the properties of the composite material.

2.1. Materials

2.1.1. Reinforcement. The reinforcement material used is bamboo, specifically the Yushania Alpina stem. Bamboo fibers are known for their strength and stiffness, making them suitable for reinforcing the composite. The properties of bamboo fiber are shown in the following Table 1.

2.1.2. Filler. The filler material utilized is waste glass fiber. Chopped glass fibers are added to enhance the mechanical properties of the composite. These fibers are obtained from waste sources, making them a cost-effective option. The properties of E-glass fiber are shown in the following Table 2.

2.1.3. Matrix. The matrix material consists of polyester, specifically GP resin 1003, along with a hardener (catalyst). Polyester serves as the base material that holds the reinforcement and filler together, providing overall structural integrity to the composite. The properties of polyester resin are shown in the following Table 3.

2.1.4. NaOH Treatment. Sodium hydroxide (NaOH) is used as a treatment for bamboo fibers. The treatment process is shown in Supplementary Material Figure S3 and is likely used to remove impurities and improve the adhesion between the fibers and the matrix.

2.1.5. Wax (Releasing Agent). Wax is used as a releasing agent to prevent the composite from sticking to the mold during the fabrication process. It facilitates the easy removal of the composite from the mold without causing damage.

2.1.6. Other Preparation and Safety Tools. Various tools and equipment specific to composite fabrication are used, such as molds, mixing containers, brushes, gloves, and safety gear. These tools ensure proper preparation, handling, and safety during the composite creation process.

2.2. Methods. The methodology employed in this study is outlined in Figure 1. It presents a systematic flowchart that elucidates the steps undertaken to forecast the behavior of the composite material. The methodology encompasses the following key steps:

2.2.1. Gathering and Preparing Composite Materials. The first step involved procuring the necessary composite materials, including bamboo fibers, chopped glass fibers, and polyester matrix and other. These materials were carefully selected and prepared to meet the required specifications for the composite fabrication process.

Table 1: Mechanical properties of bamboo fiber [34].

Properties	Value
Tensile strength (MPa)	1140 – 230
Youngs modulus (GPa)	11–17
Elongation at break (%)	~2
Density (g/cm^3)	0.6–1.42

Table 2: Mechanical properties of E-glass fiber [34].

Properties	Value
Density (g/cm^3)	2.7
Tensile strength (MPa), @ 23°C	1725
Young's modulus (GPa), @ 23°C	72.3
Refractive index	1.557
Thermal coef. Of expansion range	5.4×10^{-6} in./in./°C
Elongation	4.8%

Table 3: Mechanical properties of polyester resin [35].

Properties	Values
Density (g/cm^3)	1.2–1.5
Young modulus (GPa)	2–4.5
Tensile strength (MPa)	40–90
Tensile elongation on at break (%)	2
Water absorption 24 h at 20°C	0.1–0.3

2.2.2. Utilizing the Response Surface (RSM) Method. The response surface method, a statistical technique, was employed to design the experimental trials [36]. This method enabled the systematic exploration of the composite material's behavior by creating a mathematical model that relates the input variables (such as weight percentages) to the desired responses (mechanical and physical properties).

2.2.3. Sample Preparation. Based on the experimental design generated by the response surface method, composite samples were prepared with varying weight percentages of bamboo fibers, chopped glass fibers, and polyester matrix. The samples were fabricated following established protocols to ensure consistency and reproducibility.

2.2.4. Experiment Execution. The fabricated composite samples were subjected to a series of tests and experiments to evaluate their mechanical and physical properties. These tests involved assessing tensile strength, flexural strength, impact resistance, water absorption, and thermal stability. The experiments were conducted meticulously to obtain accurate and reliable data.

2.2.5. Analysis of Experimental Results. The data obtained from the experiments were analyzed to derive meaningful insights into the behavior of the composite material. Statistical techniques, such as regression analysis, were employed to examine the relationships between the input variables (weight percentages) and the observed responses (mechanical and physical properties). This analysis

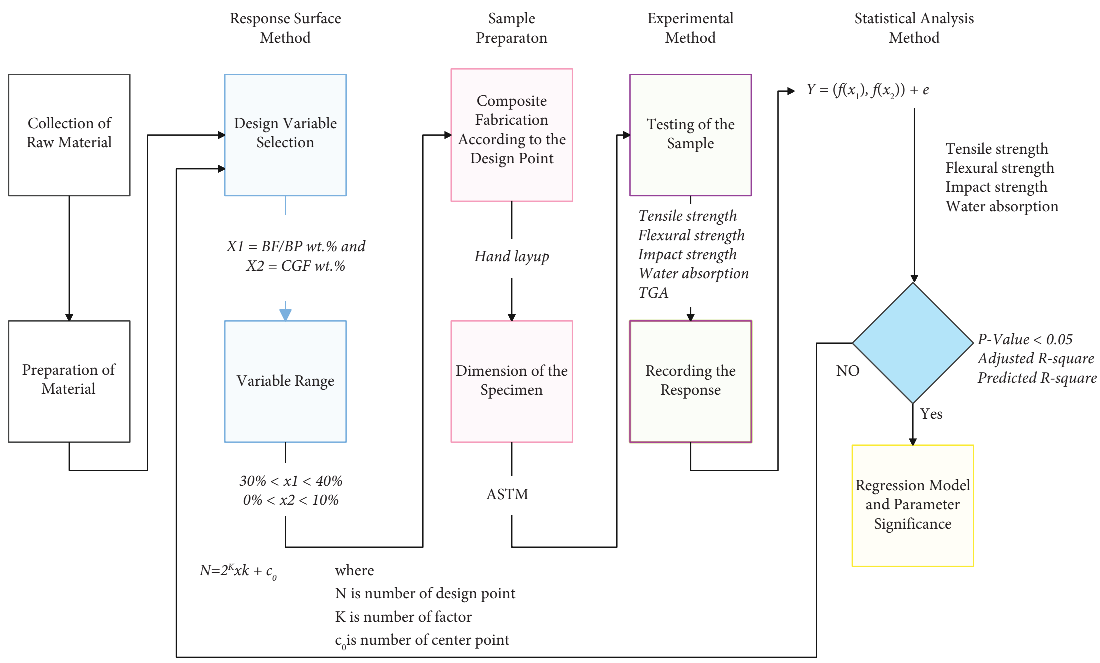

Figure 1: Methodology flowchart for the analysis of the composite.

facilitated the identification of trends, patterns, and correlations within the data.

2.2.6. Statistical Analysis. In the final step, a comprehensive statistical analysis was performed to interpret and validate the experimental results. This analysis involved techniques such as analysis of variance (ANOVA) to determine the significance of the factors and their interactions. The statistical analysis provided quantitative information on the influence of the weight percentages of the composite components on their mechanical and physical properties.

By following these steps, a robust methodology was established to forecast the behavior of the composite material. The systematic approach ensured the reliability and accuracy of the experimental data, enabling a thorough understanding of the composite's characteristics and performance.

2.2.7. Composite Preparation. This investigation employed sodium hydroxide, bamboo fiber, glass fiber, and polyester resin as the materials listed above. Sodium hydroxide often known as caustic soda, is a highly caustic metallic base and alkali salt with the chemical formula NaOH. It is a white powder that comes in pellets, flakes, granules, and a 50 percent saturated solution. NaOH was purchased from local suppliers by the brand name of CAUSTIC SODA FLAKES, as shown in Supplementary Material Figure S2.

In Ethiopia, the bamboo plant is either naturally growing or cultivated. The bamboo utilized in this study comes from an Injibara that is cultivated in the farmyard. Bamboo is gathered from this location due to the abundance of suppliers and a large number of bamboo culm available. The bamboo plant stem of a three-year-old highland bamboo (Yushania alpina) species. Bamboo fiber is obtained by water-retting bamboo strips, as shown in Supplementary Material Figure S1. The fiber was treated with NaOH and then chopped to a short (average 2 mm) fiber size that is greater than the critical length of bamboo fiber according to [37], to make short bamboo fiber-reinforced polyester random orientation. On the other hand, the long fiber is prepared in unidirectional orientation. In both cases, the fiber is treated with 5% volume fractions of NaOH concentration and soaked for 24 different hours, then washed with distilled water after that dried for an optimum hour at room temperature [38], as shown in Supplementary Material Figure S3.

In the present study, chopped-strand fiberglass mat (CSM) 300 is used as the synthetic fiber (which is an E-glass) which is made from (SiO_2: 54.3 wt.%, Al_2O_3: 15.2 wt.%, CaO: 17.2 wt.%, MgO: 4.7 wt.%, and B_2O_3: 8.0 wt.%) [39]. By milling or reducing the length of the glass fiber to a size of 0.5 to 1 mm with a milling cutter machine as shown in Supplementary Material Figure S5, waste synthetic E-glass fiber was used as filler, as shown in Supplementary Material Figure S4.

Long and short bamboo weight ratio combinations with various weight ratios of CGF were created as shown in Table 4. Different combinations were created using a weight range of bamboo fiber (30–40 wt. percent) and chopped glass fiber (0–10 wt. percent). Using this method, nine different combinations of bamboo fibers and CGF weight were created at random. The weight ratio of each combination was calculated using the mixture rule [40]. For 10 minutes, the long unidirectional or randomly oriented short fiber and chopped glass fiber were mixed with polyester in the proportions specified. The laminate was prepared using the hand layup method, and the mold used was approximately 300 mm × 240 mm × 4 mm in size as shown in Figure 2.

Table 4: Content ratio of chopped glass fiber (CGF) to long and short bamboo fiber by weight percent, respectively.

No	Short name	Bamboo fiber content (wt.%)	Chopped glass fiber filler (CGF) content (wt.%)
1	BF/BP 1	30	0
2	BF/BP 2	30	5
3	BF/BP 3	30	10
4	BF/BP 4	35	0
5	BF/BP 5	35	5
6	BF/BP 6	35	10
7	BF/BP 7	40	0
8	BF/BP 8	40	5
9	BF/BP 9	40	10

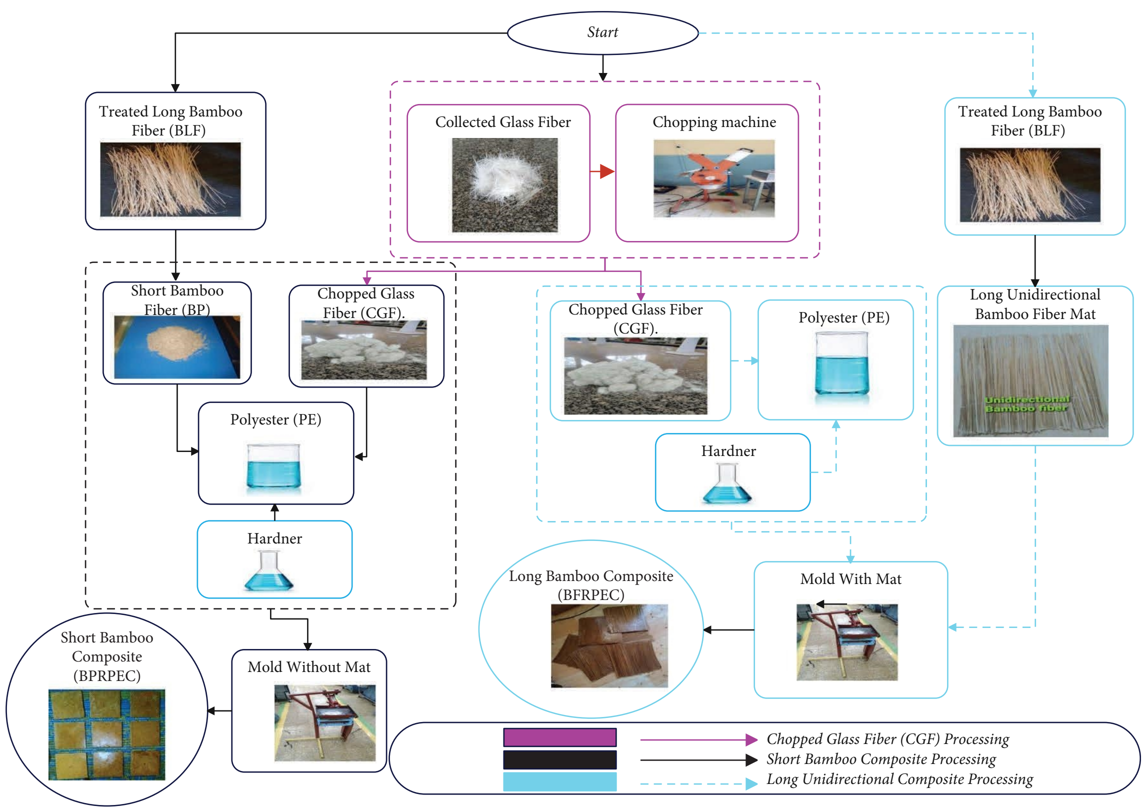

Figure 2: Methods of creating a composite sample consisting of both BFRPEC and BPRPEC with chopped glass fiber (CGF).

Molds with dimensions of 300 mm × 240 mm × 4 mm for the production of specimens were used. Wax was added to the mold surfaces to facilitate specimen removal. Before composite manufacture, the molds were cleaned to eliminate any leftover polymeric material on the mold's surface. Bamboo fiber and particulate chopped glass fiber were incorporated into the polyester matrix in varying proportions, as categorized in the range of 30–40 weight percent (wt.%) proportion of bamboo fiber and varying proportion of CGF at 0–10 wt.%, as represented in Table 4.

Hand layup molding was used to produce BF/BP and CGF filler-reinforced polyester composites. Specimens were compressed at room temperature for a period of 24 hr. while employing 1TON uniform pressure. Wax was applied on the mould surface for easy removal of the plate [41].

2.2.8. Experimental Setup

(1) Tensile Strength and Modulus. The laminate was cut according to ASTMD3039 [42], which is sample specimen dimensions of 250 mm × 20 mm × 4 mm standards for tensile as shown in Supplementary Material Figure S8. The specimens were exposed to tension and universal testing equipment as shown in Supplementary Material Figure S6 in line with the ASTMD3039 tensile technique to determine ultimate tensile strength and elastic modulus. Specimens were assessed as per [42] at room temperature (27°C) by applying a changing load cell. Tensile characteristics were estimated using specimens with a gauge length of 170 mm were used in estimating the tensile properties. Three specimens were evaluated for each design point, and their average was presented

for each sample. The dimension of a specimen is 250 mm × 20 mm × 4 mm.

(2) Flexural Strength and Modulus. The flexural specimen dimension of the test sample was according to ASTMD790 [43], which is sample specimen dimensions of 250 mm × 20 mm × 4 mm as shown in Supplementary Material Figure S9. The composites developed were investigated by exposing the sample to a three-point bending load with the help of a UTM, as shown in Supplementary Material Figure S6 with ASTM D790 [43]. Flexural properties were probed at room temperature while adopting a 5 mm/min crosshead speed and a constant strain rate to fracture three specimens of 170 mm × 20 mm × 4 mm dimension to obtain the average value for each weight fraction or ratio.

(3) Charpy Impact Strength. The ASTM D6110-10 [44] standard will be used to measure the impact strength using a Charpy impact tester with an unnotched specimen at the Strength of Materials Laboratory, Department of Mechanical Engineering, Bahir Dar University. The dimensions of the specimens were as per ASTM D6110-10 which was 127 mm × 12.7 mm × 4 mm, as shown in Supplementary Material Figure S10. This test determines how much energy a material can absorb in total. This absorption of energy is related to the material's brittleness. An impact test was used to evaluate the toughness of the bamboo and chopped glass fiber composite reinforced polyester composite. Three identical specimens were subjected to an impact test as per ASTM D6110-10 [44] using a Charpy impact testing machine as shown in Supplementary Material Figure S7. Samples were clamped to fracture samples, and the impact energy and toughness of three specimens were measured and their averages were taken. The dimension of the specimen was 127 mm × 12.7 mm × 4 mm.

(4) Water Absorption. The water absorption tests for both long and short bamboo fiber-reinforced polyester with chopped glass fiber composites were performed as per ASTM D570 [45]. At ambient temperature (20–25°C) for 24 hours until equilibrium, an oven-dried specimen of ASTM D570 dimensions was immersed in distilled water [45]. The water retention test was performed using an oven-dried test specimen of ASTM D570 dimensions which is 76.2 mm × 25.4 mm × 4 mm, as shown in Supplementary Material Figure S11 submerged in water at room temperature (20–25°C) for 24 hours until equilibrium. The specimen was taken out, dried with a cloth, and weighed on a digital weighing balance. The weight of the dry weight before (W_o) and after (W_t) immersion was noted. The percentage of water absorption (Mt) was determined.

The water uptake (M_t)

$$M_t = \frac{W_t - W_o}{W_o} \text{x}\, 100\%, \quad (1)$$

where W_o and W_t. are the weights at the initial (dry condition) and after the immersion time *t*, respectively.

(5) Thermogravimetric Analysis (TGA). In a temperature range of 25°C to 800°C, the TGA analysis was performed at a heating rate of 25°C/min on three replicas of a 10 mg sample at the Bahir Dar University Faculty of Chemical Engineering Organic Lab, as shown in Supplementary Material Figure S12. This was done to check the effect of chopped glass fiber on the properties of long bamboo fiber-reinforced polyester (BFRPEC) with or without filler and used to investigate the response to heating.

In this case, two types of composite are considered, and both statistical and experimental analysis were performed. The types of composites are long bamboo fiber and short bamboo fiber-reinforced polyester (BFRPEC and BPRPEC) with chopped glass fiber (CGF) filler.

3. Results and Discussion

3.1. Experimental Analysis of Tensile Strength. The behavior of the developed long bamboo and short bamboo fiber with chopped glass fiber (CGF) filler-reinforced polyester composites under tensile loading is presented as shown in Figures 3 and 4, respectively. Variations of bamboo fiber and chopped glass fiber filler loading or weight effect on the tensile behavior of the composites were studied. As shown in Figures 3 and 4 stress at first increased linearly then decreased rapidly above ultimate strength in the stress-strain curve that is a similar graph of brittle material, i.e., stress decreasing sharply and having ultimate tensile strength equal to yield strength.

As it is illustrated in Figure 5(a) the tensile strength of long bamboo fiber-reinforced polyester increases with Chopped glass fiber weight in each different bamboo content.

In Figure 5(a), adding 5 wt.% chopped glass fiber (CGF) filler to long bamboo fiber-reinforced polyester composites improved their tensile strength and modulus. The CGF-filled composites showed higher ultimate tensile strength and modulus compared to the unfilled composites, attributed to factors like optimal filler dispersion and fiber filler interactions.

In Figure 5(b), including 10 wt.% chopped glass filler in short bamboo fiber-reinforced polyester composites increased their tensile strength and modulus. The improved compatibility between fibers and matrix, along with enhanced wettability, led to better adherence and restricted dislocation movement. These enhancements make the composites suitable for applications requiring superior mechanical performance.

The increase might be due to the fiber and filler chopped coalescing [46]. The adherence of the filler and short bamboo fibers to the matrix was improved by their wettability, which inhibited dislocation movement [47]. With the addition of 10 wt.% CGF, the tensile strength which may be attributed to the improved compatibility between fiber and matrix as well as appropriate CGF filling.

Similar findings were observed in previous studies, such as the study conducted by Ojha et al. [25, 48] that investigated the mechanical properties of e-glass/polyester and glass fiber-reinforced polyester composites for marine

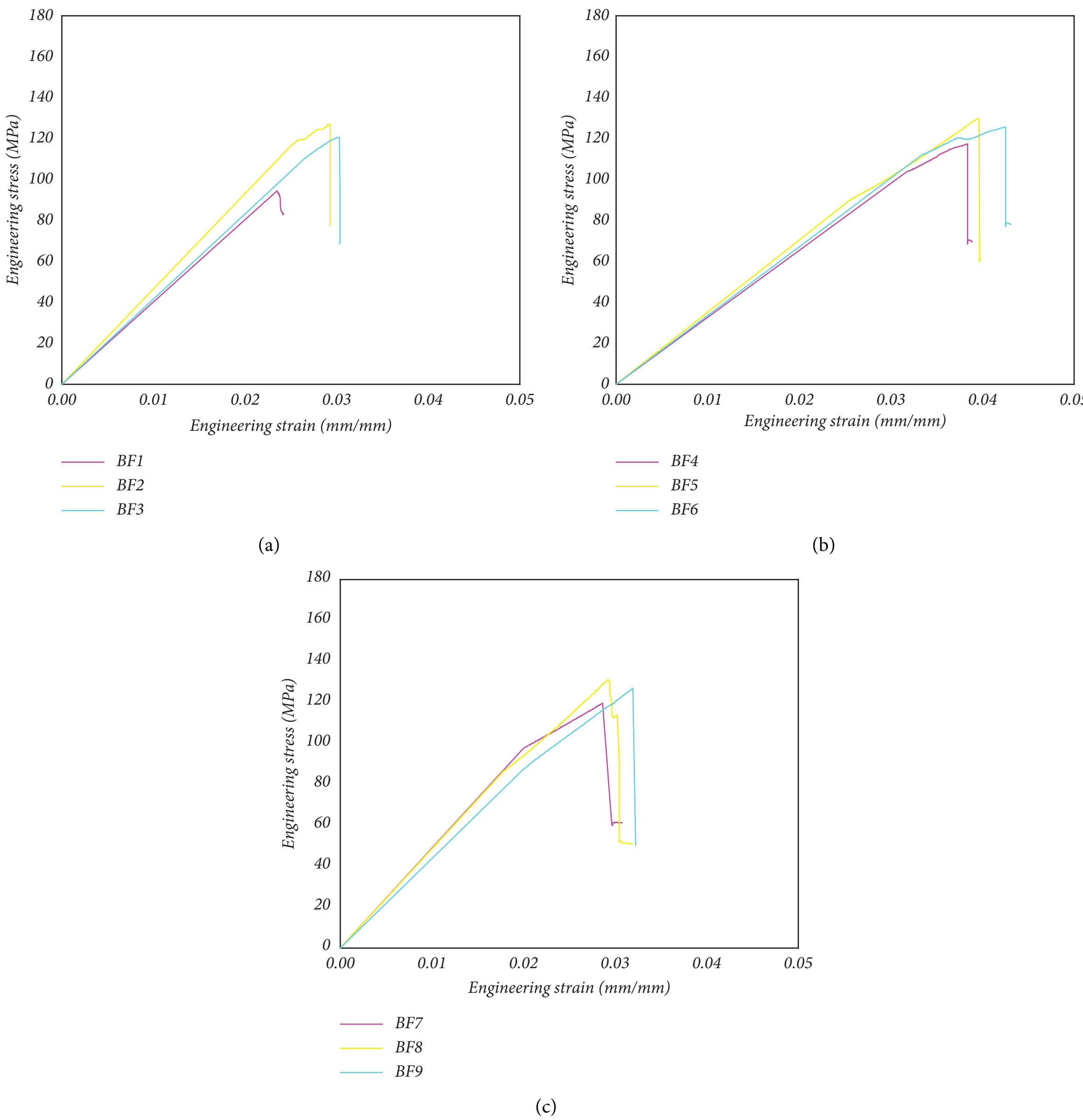

Figure 3: Strain-stress curve for BFRPEC tensile strength at (a) 30 wt.% bamboo fiber content (b) 35 wt.% bamboo fiber content (c) 40 wt.% bamboo fiber content with different content of CGF.

applications, respectively. Both studies examined the tensile, compressive, and flexural properties of the composites. The results showed that the tensile strength and modulus of the composites increased with increasing fiber content similar to this study. But the fiber content increase showed more increment in this study.

3.2. Statistical Analysis of Ultimate Tensile Strength. The quadratic models for ultimate tensile strength in BFRPEC showed significant P-values (<0.05), high R-squared, adjusted R-squared, and predicted R-squared values, as evidenced in Table 5 and Figures 6(a) and 6(b). The regression equations (2) and (4) contained only significant factors (as x_1, x_2 and $x_2{}^2$) with P-values <0.05. The agreement between actual and predicted results in Figure 7(a) supports the model's predictive capability.

In contrast, for BPRPEC ultimate tensile strength, both linear and quadratic models demonstrated good P-values, R-squared, adjusted R-squared, and predicted R-squared values. The obtained result, as shown in Table 6 and Figures 8(a) and 8(b), demonstrated a strong p value for the linear model in the regression equations (3) and (5). The Predicted R^2 (0.9292) closely aligned with the Adjusted R^2 (0.9597), indicating a difference of less than 0.2. The high precision ratio (25.7804) indicated an adequate signal. The agreement between actual and predicted results in Figure 9(a) further supports the model's predictive accuracy.

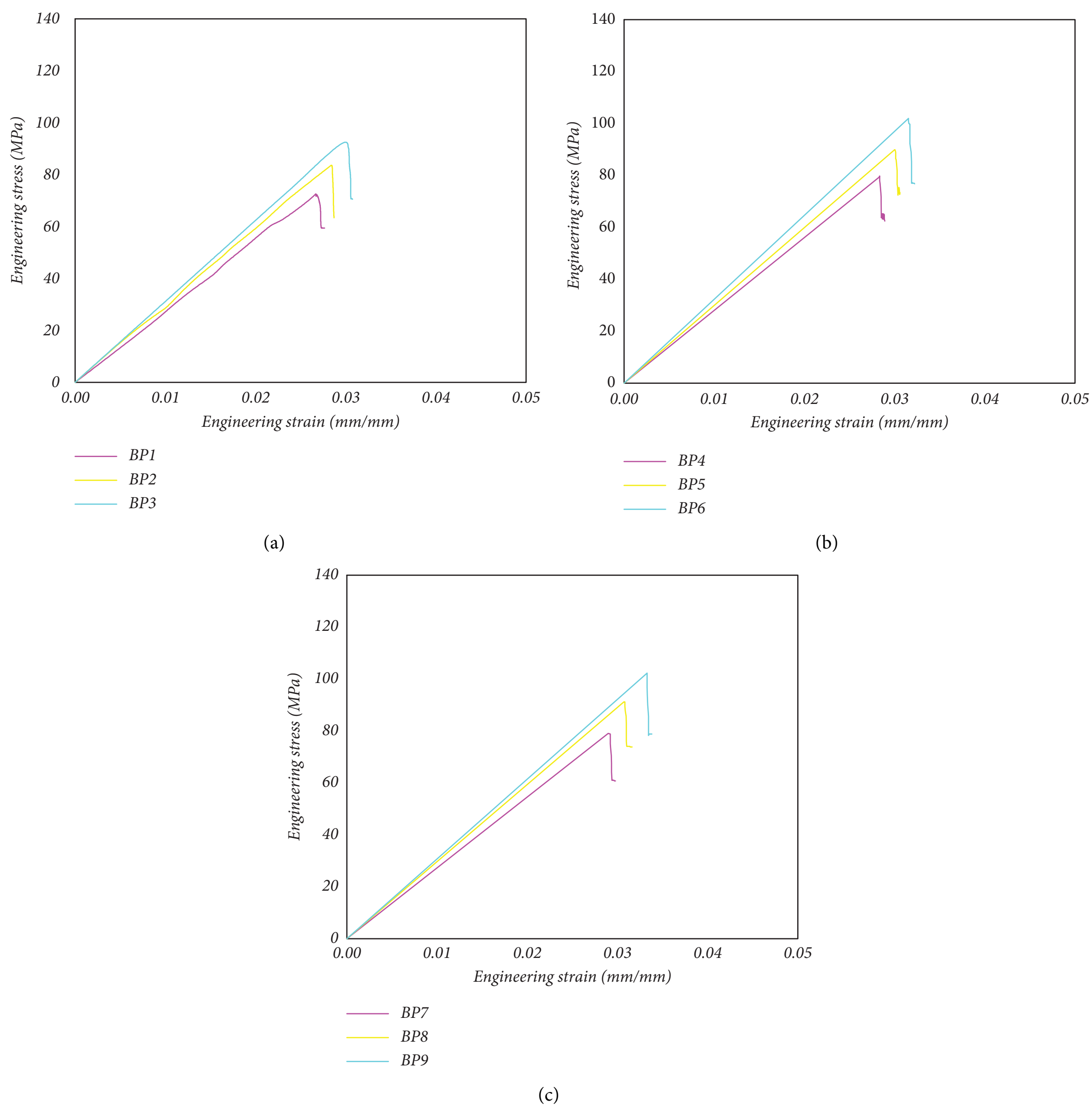

FIGURE 4: Strain-stress curve for BPRPEC tensile strength at (a) 30 wt.% bamboo fiber content (b) 35 wt.% bamboo fiber content (c) 40 wt.% bamboo fiber content with different content of CGF.

Overall, the quadratic models performed well for BFRPEC, while the linear model showed promise for BPRPEC, both in predicting ultimate tensile strength in bamboo fiber composites with varying chopped glass fiber contents.

Coded Regression Model

$$\text{Ultimate Tensile strength (BFRPEC)} = +130.23 + 4.73x_1 + +10.19x_2 - 15.04{x_2}^2, \tag{2}$$

$$\text{Ultimate Tensile strength (BPRPEC)} = 88.5206 + 4.184167x_1 + +9.7484x_2. \tag{3}$$

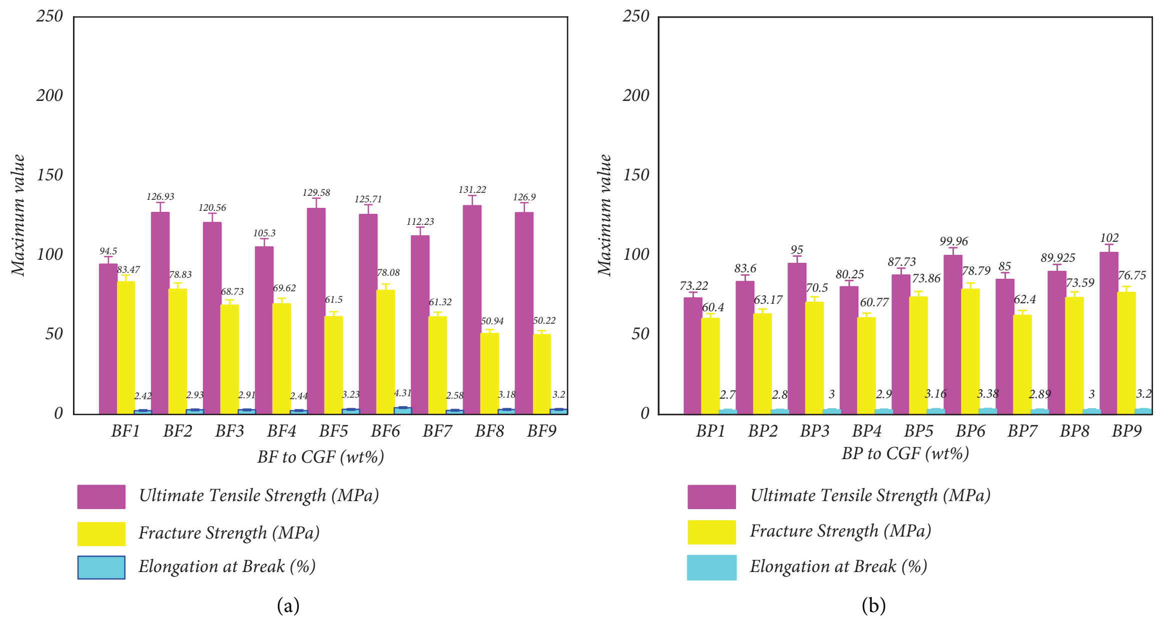

Figure 5: Ultimate strength, fracture strength, and elongation at break of (a) BFRPEC and (b) BPRPEC with CGF filler.

Table 5: ANOVA model summary for tensile strength of the BFRPEC with CGF filler.

Source	P-value	R-squared	Adjusted R-squared	Predicted R-squared	Adequate precision
Linear	0.065	0.5973	0.4631	0.1083	5.6029
Quadratic	0.0071	0.9834	0.9559	0.8021	17.40

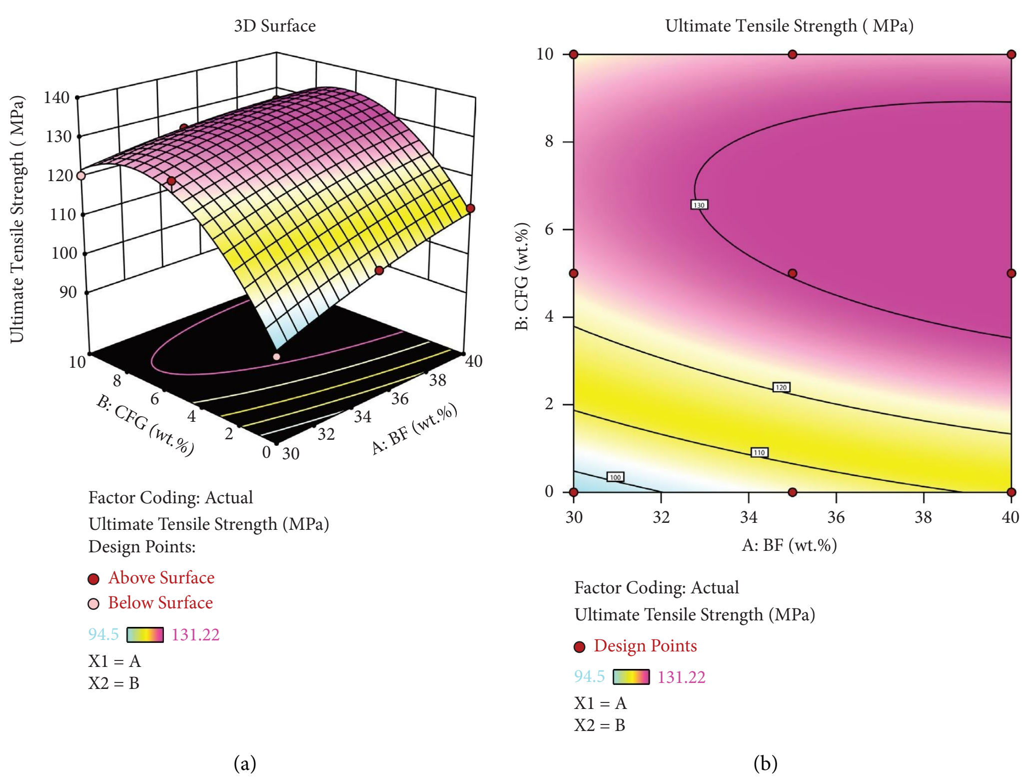

Figure 6: Continued.

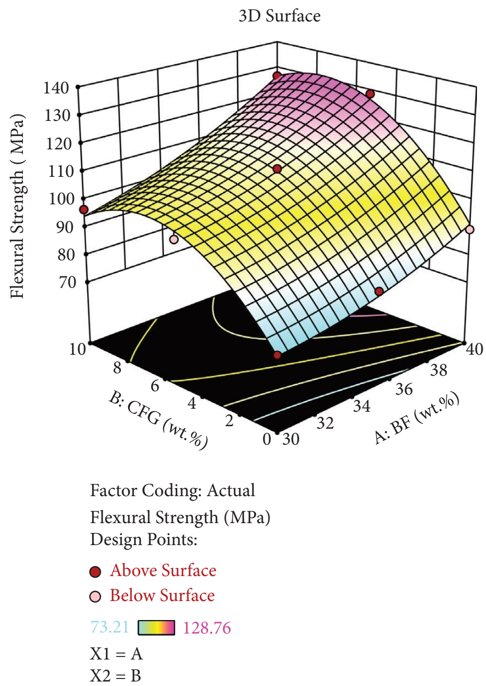

(c)

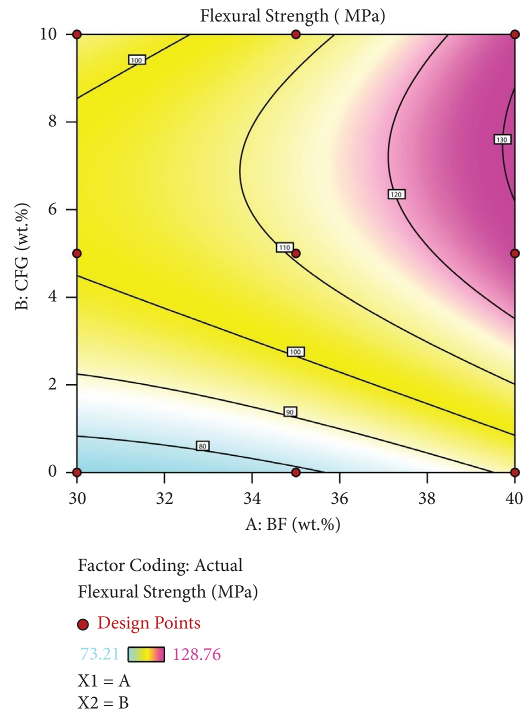

(d)

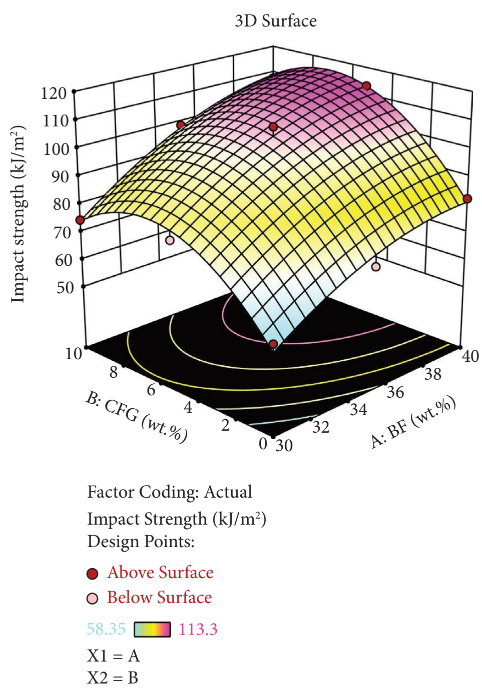

(e)

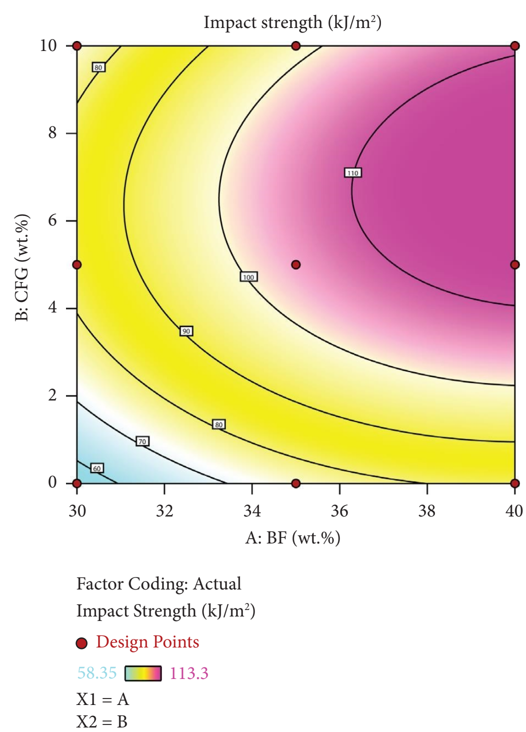

(f)

FIGURE 6: Continued.

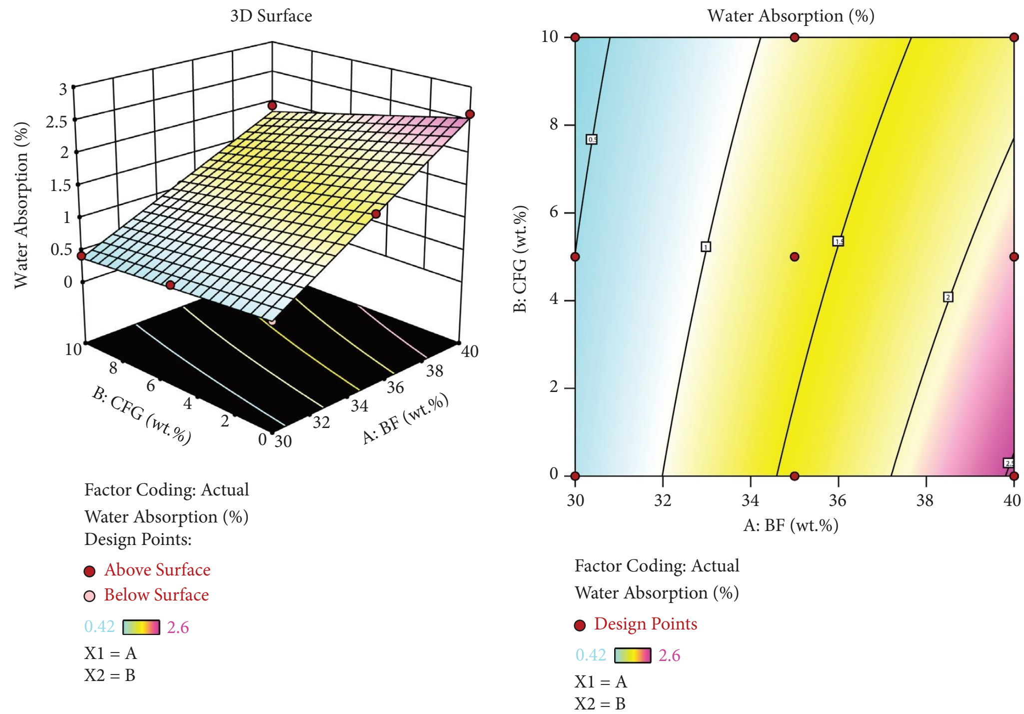

(g) (h)

Figure 6: RSM model and contour plot of BFRPEC with CGF filler for tensile (a and b), flexural (c and d), impact (e and f), and water absorption (g and h) respectively.

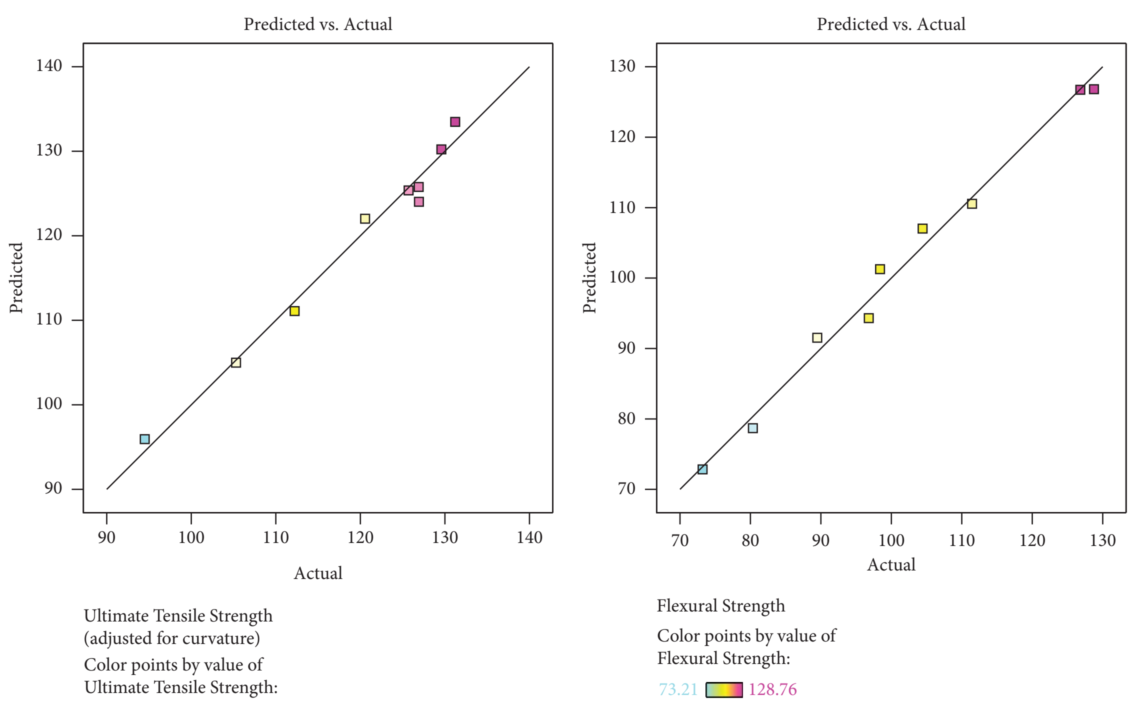

(a) (b)

Figure 7: Continued.

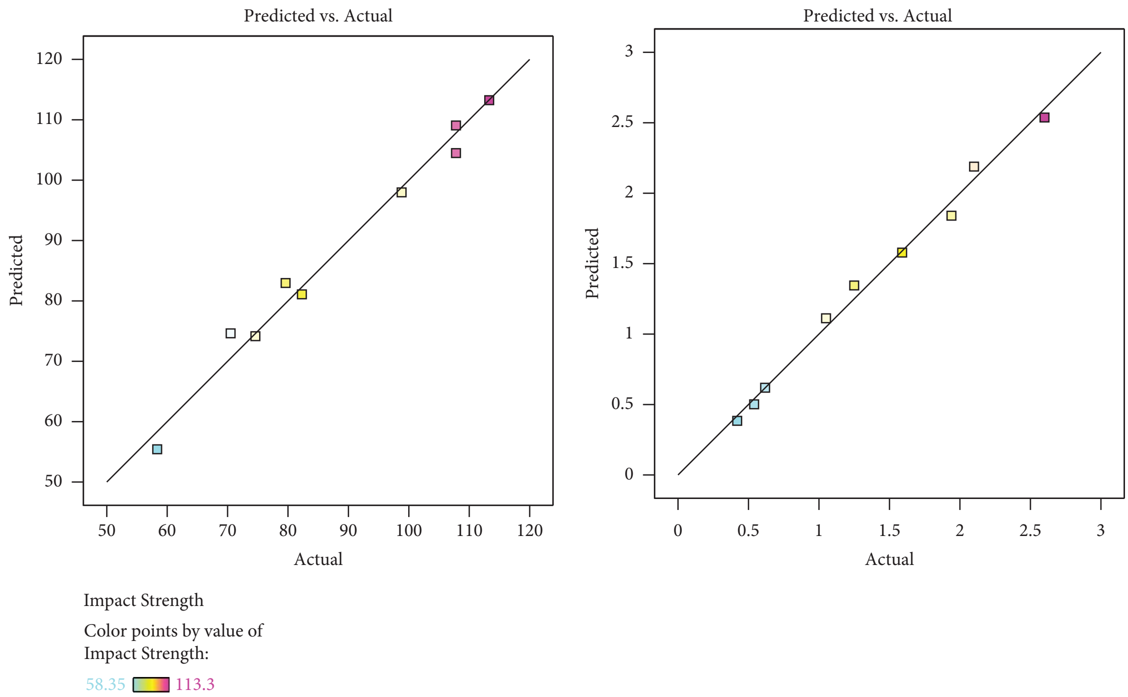

(c) (d)

Figure 7: Experimental (actual) and prediction model output for BFRPEC with CGF filler (a) tensile, (b) flexural, (c) impact, and (d) water absorption respectively.

Table 6: ANOVA model summary for tensile strength of BPRPEC with CGF filler.

Source	P-value	R-squared	Adjusted R-squared	Predicted R-squared	Adequate precision
Linear	0.0001	0.9698	0.9597	0.9292	25.7804
Quadratic	0.0011	0.9954	0.9877	0.9440	32.9683

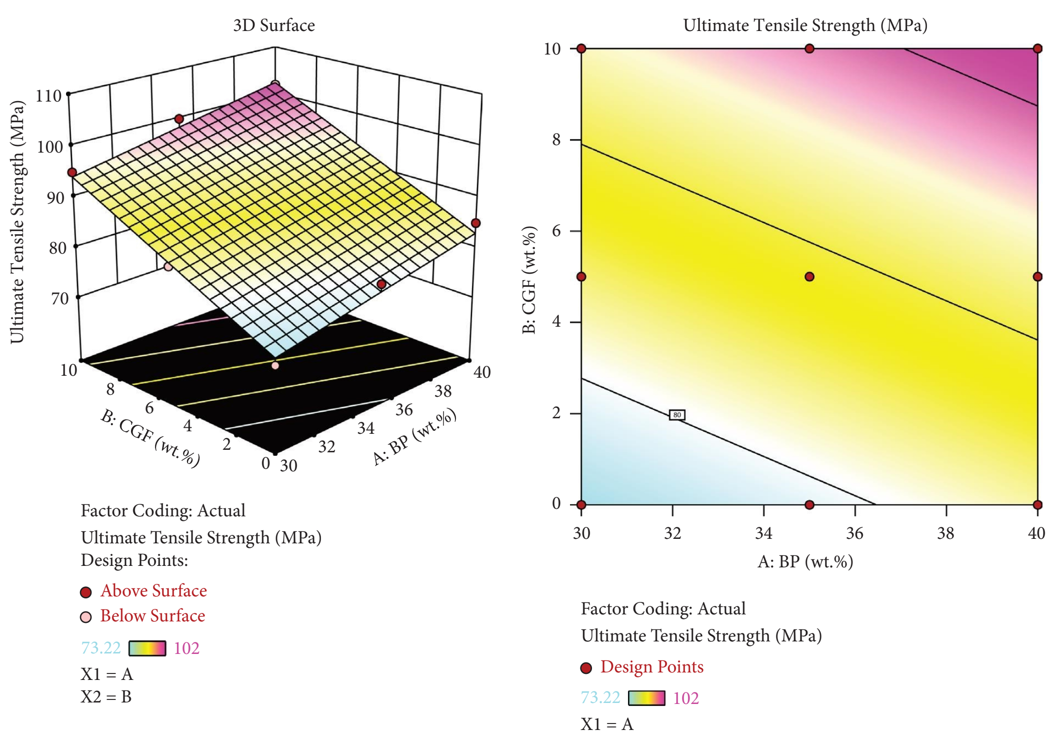

(a) (b)

Figure 8: Continued.

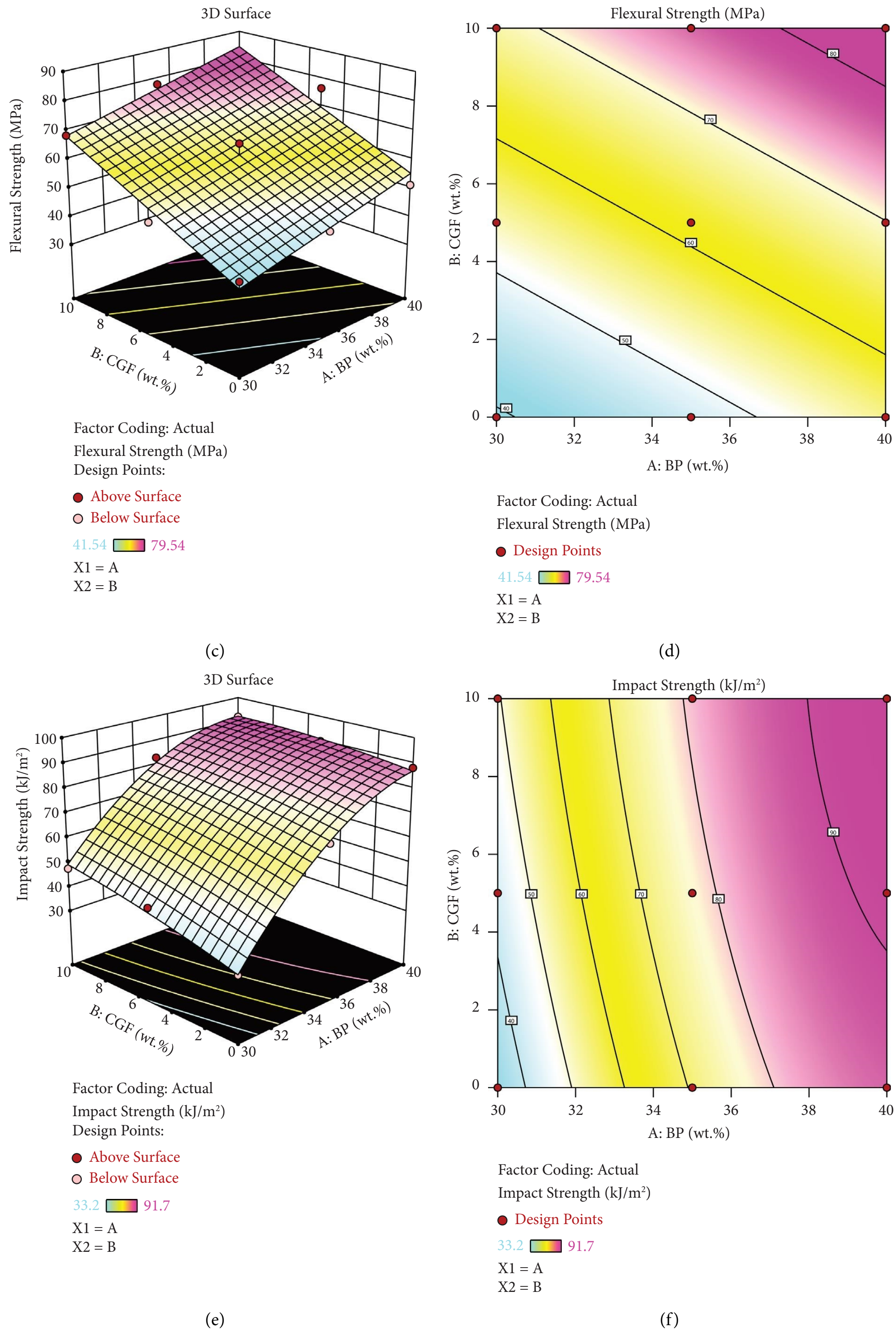

Figure 8: Continued.

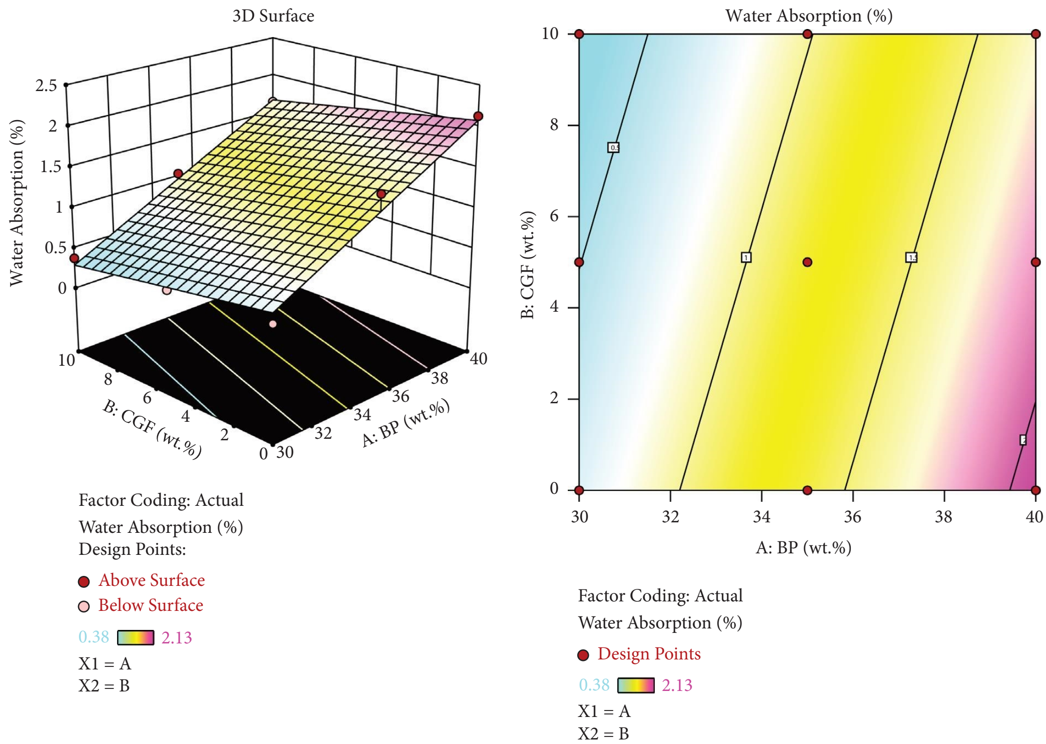

(g) (h)

Figure 8: RSM model and contour plot of BPRPEC with CGF filler for tensile (a and b), flexural (c and d), impact (e and f), and Water absorption (g and h) respectively.

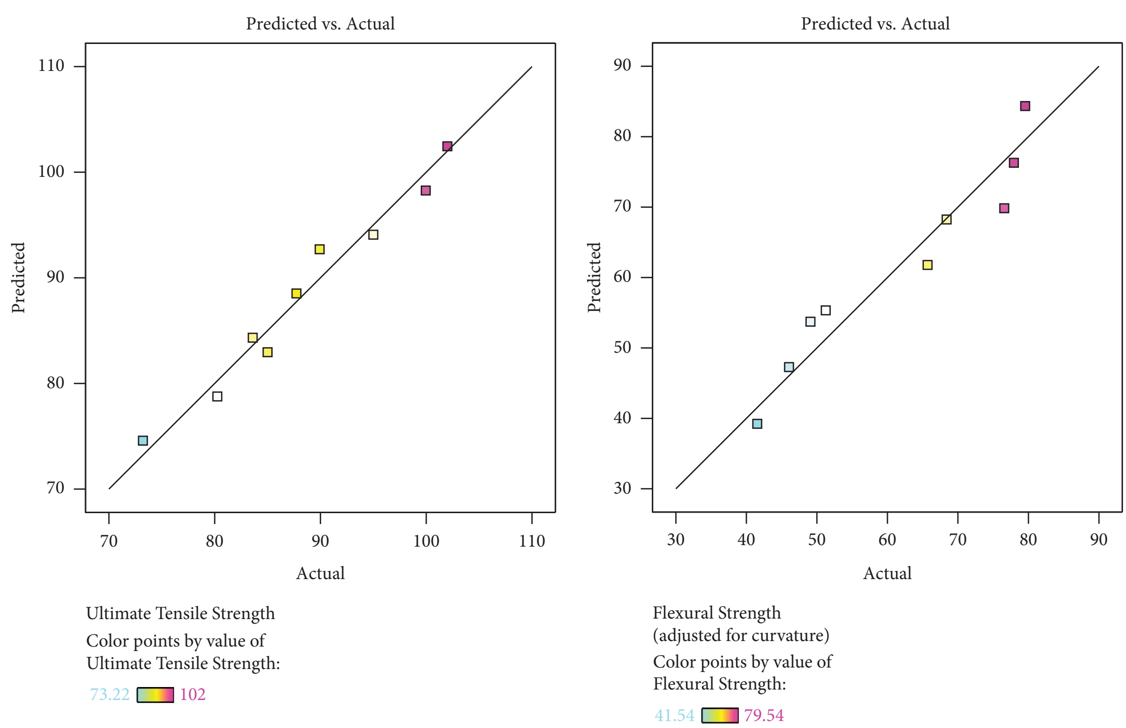

(a) (b)

Figure 9: Continued.

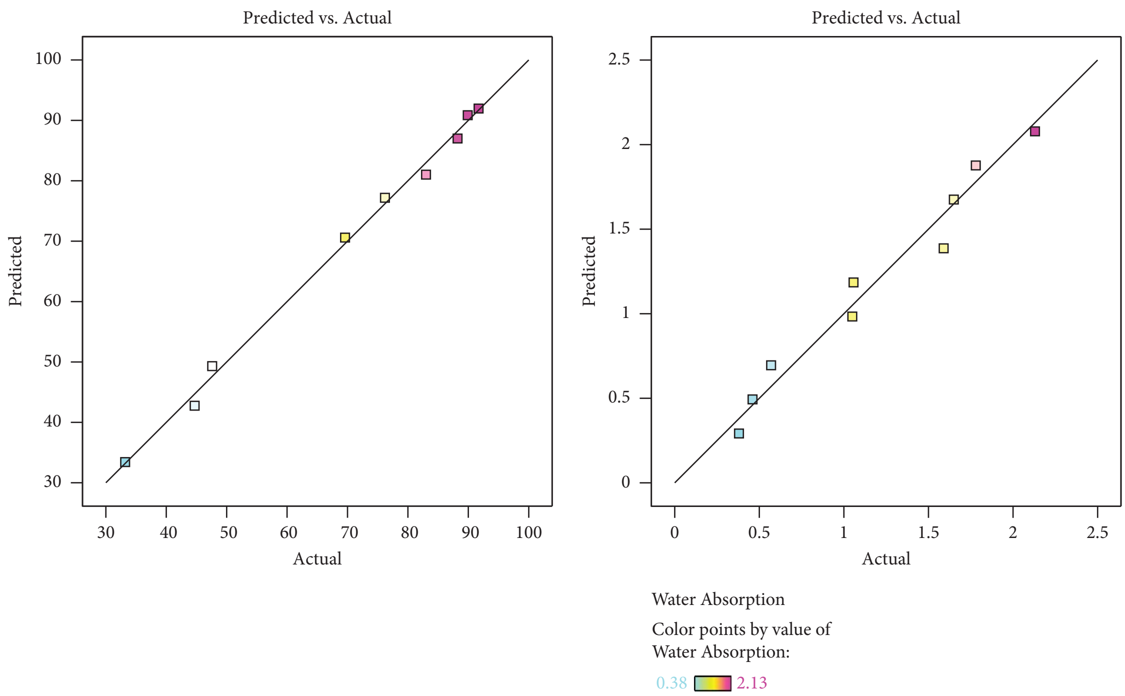

(c) (d)

Figure 9: Experimental (actual) and prediction model output for BPRPEC with CGF filler (a) tensile, (b) flexural, (c) impact, and (d) water absorption respectively.

Actual Regression Model

$$\text{Ultimate Tensile strength (BFRPEC)} = -20.22028 + 5.6401\text{BF wt\%} + 12.04183\text{CGF wt\%} - 0.601733\text{CGF wt\%}^2, \quad (4)$$

$$\text{Ultimate Tensile strength (BPRPEC)} = 49.48306 + 0.83684\text{BP wt.\%} + 1.9497\text{CGF wt.\%}, \quad (5)$$

where x_1: -is long/short bamboo fiber weight (BF/BP wt.%), x_2: -is chopped glass fiber weight (CGF wt.%)

3.3. Experimental Analysis of Flexural Strength. The behavior of the developed long and Short bamboo fiber with chopped glass fiber (CGF) filler-reinforced polyester composites under flexural loading is presented as shown in Figures 10 and 11 respectively. The addition of CGF filler to the BFRPEC/BPRPEC significantly improved the composite flexural strength according to the experimental result obtained from the universal testing machine (UTM) upon three points bending at the middle of the span length of the specimen prepared.

In Figure 12(a), the addition of 5 wt.% chopped glass fibers (CGF) significantly enhanced the flexural strength of long bamboo fiber-reinforced polyester composites (BFRPEC) at BF2, BF5, and BF8 composite samples. The flexural strength and modulus showed improvement compared to the unfilled composites and those with 10 wt.% CGF. This enhancement was attributed to the collaborative effect between long bamboo fibers and CGF, which improved bonding, dispersion, and reinforcement network, leading to better load transfer and stress distribution. BFRPEC with 5 wt.% CGF demonstrated potential for high-performance applications. Notably, the flexural strength increased with increasing fiber loading, particularly with the addition of 5 and 10 wt.% CGF, which resulted from bamboo fiber and CGF agglomeration. The inclusion of 5 wt.% CGF significantly increased the flexural strength value at a fiber loading of 40 wt.%.

In Figure 12(b), incorporating 10 wt.% chopped glass filler into 30 wt.% short bamboo-reinforced polyester composites (BPRPEC) improved the flexural strength and modulus compared to the unfilled composite and the composite with 5 wt.% chopped glass fiber. Similarly, for the 35 wt.% BPRPEC with 10 wt.% chopped glass filler, there was an increase in tensile strength and modulus compared to the unfilled composite and the composite with 5 wt.% chopped glass fiber. The flexural strength and modulus were further enhanced in the 40 wt.% BPRPEC with 10 wt.% chopped glass filler. These results demonstrated the improved mechanical properties achieved through the addition of 10 wt.% chopped glass filler in BPRPEC.

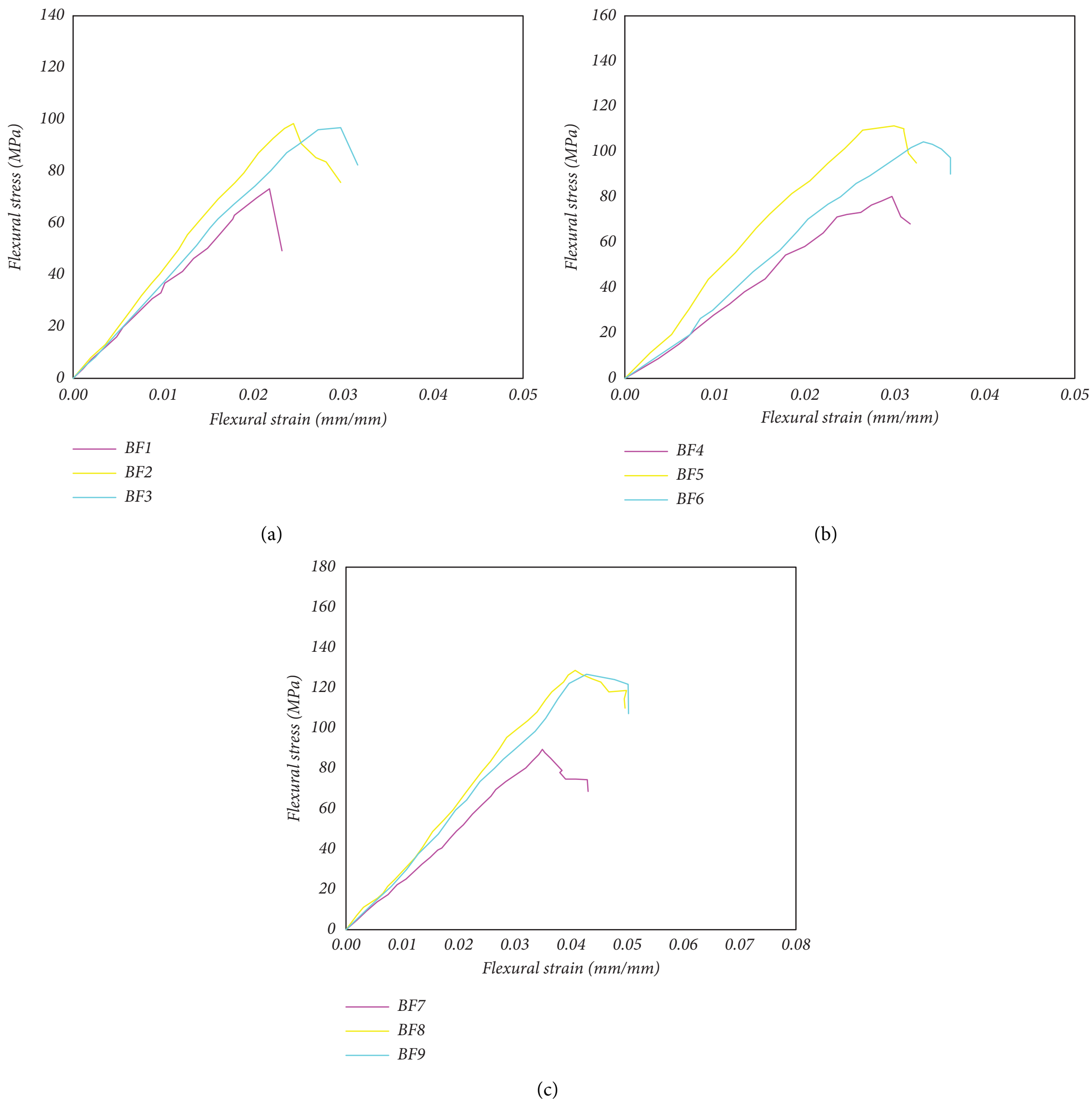

Figure 10: Strain-stress curve of flexural strength at (a) 30 wt.% (b) 35 wt.% (c) 40 wt.% bamboo fiber content of BFRPEC with chopped glass fiber filler.

3.4. Statistical Analysis of Flexural Strength. For the flexural strength of BFRPEC, both the linear and quadratic models demonstrated good *P*-values, *R*-squared, adjusted *R*-squared, and predicted *R*-squared values. However, the quadratic model exhibited a higher value of adequate precision, making it the better predictive model, as indicated in Table 7 and Figures 6(c) and 6(d). The *P*-values for both linear and quadratic models were highly significant. The precision ratio for all models confirmed their adequacy, with the quadratic model showing the highest precision. The regression equation for flexural strength (equations (6) and (8)) included only important components, namely x_1, x_2 and ${x_2}^2$. The Predicted R^2 (0.8661) closely aligned with the Adjusted R^2 (0.97), with a difference of less than 0.2. The agreement between actual and predicted results in Figure 7(b) further supports the model's accuracy in predicting flexural strength.

Regarding the flexural strength of BPRPEC, both linear and quadratic models also showed good values for *P*-value, *R*-squared, adjusted *R*-squared, and predicted *R*-squared, with the linear model exhibiting a higher value and adequate precision, as shown in Table 8 and Figures 8(c) and 8(d). The agreement between actual and predicted results in Figure 9(b) indicates a small difference and supports the model's predictive capability for each bamboo fiber content with different chopped glass fiber contents. The regression equation for flexural strength (equations (7) and (9)) included only important components.

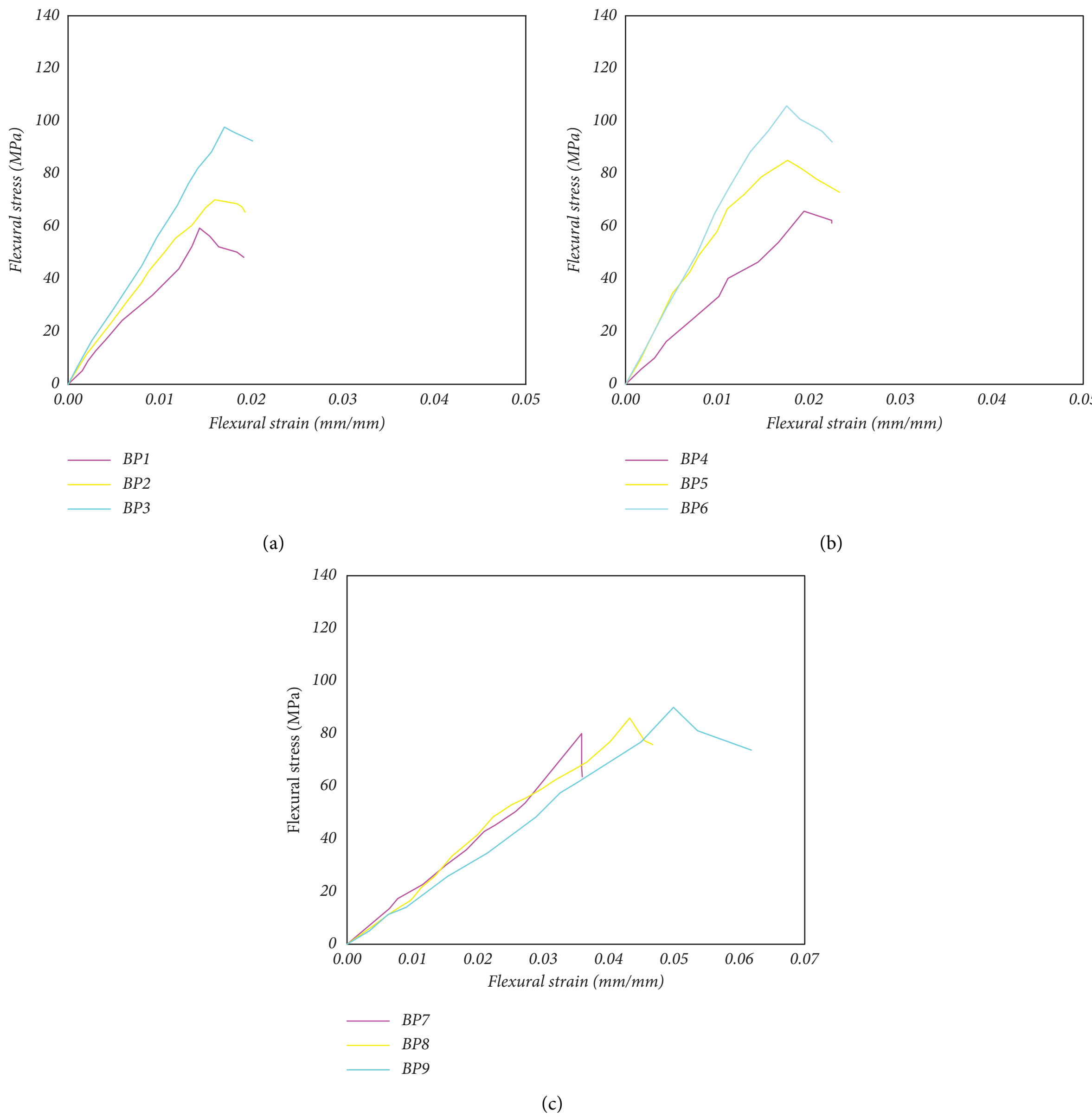

Figure 11: Strain-stress curve of flexural strength at (a) 30 wt.% (b) 35 wt.% (c) 40 wt.% bamboo fiber content of BPRPEC with chopped glass fiber filler.

Coded Regression Model

$$\text{Flexural strength (BFRPEC)} = +110.54 + + 12.78x_1 + 14.17x_2 + -17.69{x_2}^2, \tag{6}$$

$$\text{Flexural strength (BPRPEC)} = +61.787 + 8.055x_1 + 14.507x_2. \tag{7}$$

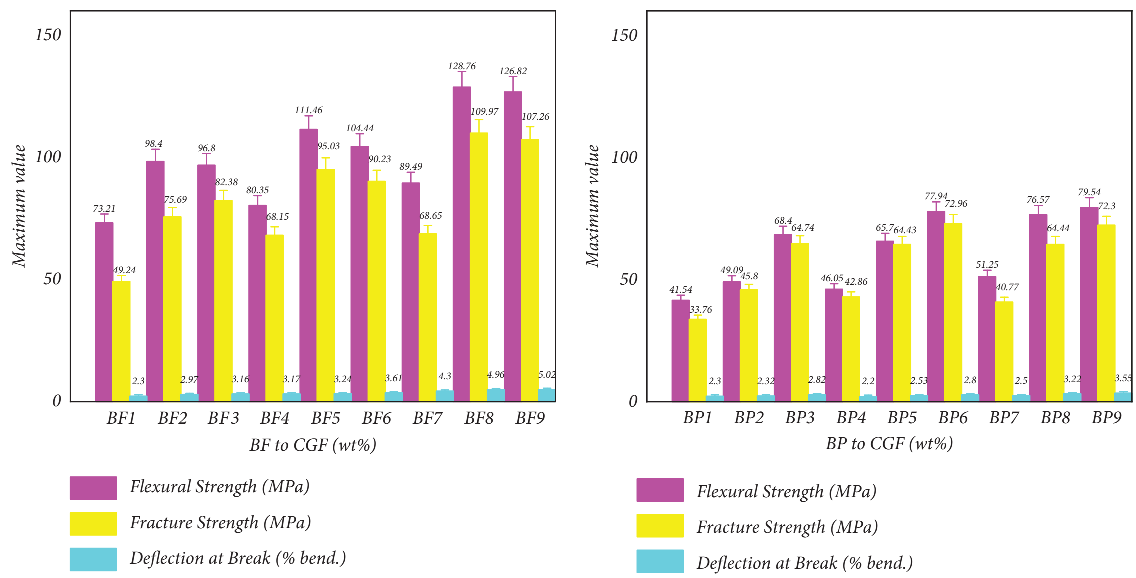

(a) (b)

Figure 12: Flexural strength, fracture strength, and strain at fracture of (a) BFRPEC and (b) BFRPEC with CGF filler.

Table 7: ANOVA model summary for flexural strength of BFRPEC with CGF filler.

Source	P-value	R-squared	Adjusted R-squared	Predicted R-squared	Adequate precision
Linear	0.01573	0.7494	0.6659	0.48083	8.4613
Quadratic	0.04	0.9888	0.97	0.8661	20.0079

Table 8: ANOVA Model summary for flexural strength of BPRPEC with CGF filler.

Source	P-value	R-squared	Adjusted R-squared	Predicted R-squared	Adequate precision
Linear	0.0004	0.9262	0.9017	0.8307	16.69
Quadratic	0.0451	0.941	0.845	0.2927	9.401

Actual Regression Model

$$\text{Flexural strength }(BFRPEC) = +184.63056 - 7.92233\text{BFwt\%} + 5.10000\text{CGFwt\%} + 0.137400\text{BFwt\%} * \text{CGF wt\%} + 0.139867\text{BFwt\%}^2 - 0.707533\text{CGFwt\%}^2, \quad (8)$$

$$\text{Flexural strength (BPRPEC)} = -9.105 + 1.611\text{BPwt\%} + 2.9013\text{CGFwt\%}. \quad (9)$$

3.5. Experimental Analysis of Impact Strength. The impact strength of the composites developed using long bamboo fibers and CGF filler, as presented in Table 9 and Figure 13, exhibited an increasing trend with fiber loading ranging from 30 to 40 wt.% and 0–10 wt.% CGF content. The Charpy impact test results in Table 9, which included three specimens tested for the same content, showed close proximity between the results and the average value, as indicated by the small standard deviation. This suggests that the obtained results are acceptable. Notably, the experiment with BF4, which had the smallest standard deviation of 0.113, demonstrated good experimental performance, with all specimens closely aligned with the average value. On the other hand, BF6 exhibited the highest standard deviation of 0.9, indicating a larger deviation of one experimental result from the average compared to other experiments. However, overall, all experiments showed low standard deviation, indicating good experimental quality since they were close to the average values.

Similar to other mechanical properties, the impact strength of bamboo-reinforced polyester composites is enhanced by the addition of chopped glass fiber and increasing the weight of bamboo fiber. The impact strength, which serves as a measure of material toughness, is influenced by both reinforcement and filler. Table 9 presents the impact strength of composites with varied contents of chopped glass

Table 9: Impact toughness of different long bamboo fiber (BF) and CGF content along with a replica of the test sample.

Sample	BFRPEC toughness (kJ/m^2)				Standard deviation
	Specimen 1	Specimen 2	Specimen 3	Average	
BF1	58.15	58.4	58.5	58.35	0.18
BF2	78.31	80.06	80.43	79.6	1.132
BF3	74.34	75	74.46	74.6	0.3515
BF4	70.45	70.42	70.63	70.5	0.113
BF5	107.72	108.72	106.96	107.8	0.8827
BF6	83.02	82.59	81.29	98.8	0.9
BF7	81.8	82.9	82.2	82.3	0.556
BF8	112.9	113.88	113.12	113.3	0.514
BF9	107.72	107.18	108.5	107.8	0.663

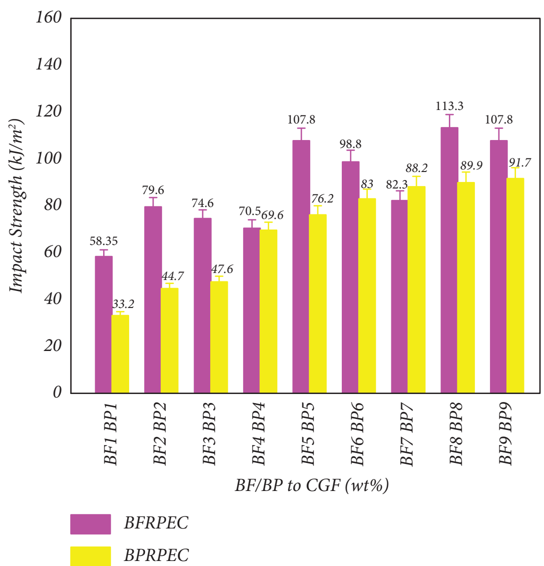

Figure 13: Impact toughness of BFRPEC and BPRPEC at different content of bamboo fiber and CGF filler.

fiber and long bamboo fiber reinforcement (30%, 35%, and 40% weight percentages). Similarly, Table 10 illustrates the impact strength of composites with varied contents of chopped glass fiber and short bamboo fiber reinforcement (30%, 35%, and 40% weight percentages). In the case of BPRPEC, the maximum impact toughness of 91.7 kJ/mm^2 was achieved with 5 wt.% chopped glass fiber content at each 30%, 35%, and 40% bamboo fiber content, specifically at BF9. However, for BPRPEC, the highest impact strength was observed at BP3, BP6, and BP9 in Table 10, due to the higher concentration of chopped glass fibers in those samples.

3.6. Statistical Analysis of Impact Strength. The impact energy of BFRPEC was analyzed using linear and quadratic models, both of which exhibited good *P*-values, *R*-squared, and adjusted *R*-squared values. However, only the linear model demonstrated a difference of less than 0.2 between the adjusted *R*-squared and predicted *R*-squared, as shown in Table 11 and Figures 6(c) and 6(d). The *P*-values for both linear and quadratic models were within the significant level. The precision ratios for all models were adequate, with the linear model having the highest precision. Hence, the quadratic model was chosen as the best model for predicting impact energy, with a prediction precision of 82.8%. The agreement between the actual and model-predicted results, as depicted in Figure 7(c), showcased a small difference, indicating the model's capability for accurate prediction. The regression equation for impact strength (equations (10) and (12)) included only important components.

Similarly, for BPRPEC, the impact energy was analyzed using linear and quadratic models, both of which demonstrated good *P*-values, *R*-squared, and adjusted *R*-squared values. However, only the linear model exhibited a difference of less than 0.2 between the adjusted *R*-squared and predicted *R*-squared, as shown in Table 12 and Figures 8(e) and 8(f). The agreement between the actual and model-predicted results, as depicted in Figure 9(c), displayed a small difference, further supporting the model's predictive capability for each short bamboo fiber content with varying chopped glass fiber content. The regression equation for impact strength (equations (11) and (13)) included only important components.

Coded Regression Model

$$\text{Impact strength (BFRPEC)} = 104.48 + 15.14x_1 + 11.67x_2 - 18.17{x_2}^2, \quad (10)$$

$$\text{Impact strength (BPRPEC)} = 77.19 + 24.054x_1 + 5.214x_2 - 10.38{x_1}^2. \quad (11)$$

Table 10: Impact toughness of different short bamboo fiber (BP) and CGF content along with a replica of the test sample.

Sample	BPRPEC toughness (kJ/m^2)				Standard deviation
	Specimen 1	Specimen 2	Specimen 3	Average	
BP1	33.56	33.22	32.82	33.2	0.37
BP2	44.2	44.65	45.25	44.7	0.526
BP3	47.22	47.56	48.1	47.6	0.443
BP4	69.5	68.84	70.45	69.6	0.8
BP5	75.86	76	76.61	76.2	0.398
BP6	82.95	83.68	82.36	83	0.6612
BP7	87.72	88.45	88.36	88.2	0.398
BP8	89.5	90.6	89.6	89.9	0.6
BP9	91.59	92.47	90.9	91.7	0.786

Table 11: ANOVA model summary for impact strength of BFRPEC with CGF filler.

Source	*P*-value	*R*-squared	Adjusted *R*-squared	Predicted *R*-squared	Adequate precision
Linear	0.0198	0.729	0.638	0.4559	7.969
Quadratic	0.076	0.9827	0.9540	0.8288	17.02

Table 12: ANOVA model summary for impact strength of polyester BPRPEC with CGF filter.

Source	*P*-value	*R*-squared	Adjusted *R*-squared	Predicted *R*-squared	Adequate precision
Linear	0.00031	0.932	0.909	0.842	15.27
Quadratic	0.0008201	0.996	0.989	0.95	31.89

Actual Regression Model

$$\text{Impact energy (BFRPEC)} = -327.54583333334 + 20.415833333334\ \text{BF wt\%} + 6.3675\ \text{CGF wt\%} - 0.727\text{CGF wt\%}^2, \tag{12}$$

$$\text{Impact energy (BPRPEC)} = -625.51 + 34.4207\text{BP wt\%} + 5.42\text{CGF wt\%} - 0.4152\text{BP wt\%}^2. \tag{13}$$

3.7. Experimental Analysis of Water Retention Capacity. Water absorption results for BFRPEC with varied proportions of CGF are presented in Table 13. The trend in water retention (%) showed a downward trend with increasing CGF proportion, attributed to the hydrophobic nature of CGF. This confirmed the decrease in water retention as CGF content increased, ranging from 0 to 10 wt.%, when intermixed with BF ranging from 30 to 40 wt.%. However, when 10 wt.% CGF was blended with 30%, 35%, and 40% BF, a continuous increase in water retention was observed. This can be attributed to the hydrophilic nature of BF occupying a greater space and non-bonding between the matrix and bamboo fiber due to the high filler content, resulting in increased water retention. Additionally, at this percentage, water penetration weakened the connection between the fiber and matrix, leading to fiber separation and increased water suction. Similar findings were observed in previous studies, such as Sallal [49], where the addition of bio-filler (coconut shell powder) resulted in increased water absorption of the matrix. Further support for this phenomenon can be found in references [50–53].

The water absorption experiments exhibited low standard deviations, with the smallest value of 0.0104 observed at BF2, indicating good experimental performance and close alignment of all specimens with the average value. The highest standard deviation of 0.1322 was observed at BF7, indicating a larger deviation of one experimental result from the average compared to other experiments. However, overall, all experiments showed low standard deviation, suggesting good experimental quality as they were close to the average values.

Water absorption results for BPRPEC with varied proportions of CGF are shown in Table 14. Similar to BFRPEC, water retention (%) decreased with increasing CGF content due to CGF's hydrophobic nature. This confirmed the decrease in water retention as CGF increased, ranging from 0 to 10 wt.%, when mixed with BP ranging from 30 to 40 wt.%. However, when 10 wt.% CGF was blended with 30%, 35%, and 40% BP, a continuous increase in water retention was observed. This can be attributed to the hydrophilic nature of BP occupying a greater space and non-bonding between the matrix and bamboo fiber due to the high filler content, resulting in increased water retention.

Table 13: Water absorption of BFRPEC with CGF filler content along with a replica of the test sample.

Sample	BFRPEC with CGF water absorption (%)				Standard deviation
	Specimen 1	Specimen 2	Specimen 3	Average	
BF1	0.59	0.56	0.58	0.57	0.0153
BF2	0.47	0.45	0.455	0.46	0.0104
BF3	0.385	0.39	0.365	0.38	0.0132
BF4	1.53	1.66	1.58	1.59	0.0655
BF5	1.05	1.05	1.197	1.057	0.0848
BF6	1	1	1.15	1.05	0.08487
BF7	2.65	2.45	2.7	2.6	0.1322
BF8	1.7	1.88	1.76	1.78	0.0916
BF9	1.6	1.75	1.6	1.65	0.0866

Furthermore, water penetration at this percentage weakened the connection between the fiber and matrix, leading to fiber separation and increased water absorption. As observed in Table 14, water absorption results for different contents of BP and CGF wt.% were depicted, with the lowest result found at BP3 due to the low content of short bamboo fiber and high CGF content, which further confirms their hydrophilic and hydrophobic nature, respectively.

3.8. Statistical Analysis of Water Absorption. In terms of BFRPEC water absorption, the two-factor interaction (2FI) linear model exhibited favorable values for the P-value, R-squared, and adjusted R-squared. However, the 2FI linear and quadratic models displayed a difference of less than 0.2 between the adjusted R-squared and predicted R-squared, with the 2FI linear model having P-values within the significant level. The precision ratio of all models was desirable. Consequently, the 2FI linear model was selected as the superior model for water absorption, as indicated in Table 15 and Figures 6(g) and 6(h). In Figures 6(g) and 6(h), the color gradient ranges from blue (representing the lowest water absorption) to green, yellow, orange, and red (representing the highest water absorption). Additionally, Figure 7(d) demonstrates that the actual and model-predicted results for each bamboo fiber content with different chopped glass fiber content exhibit good agreement with only minor differences, thereby indicating the model's improved predictive capability. The regression equation for water absorption (equations (14) and (16)) included only important components.

For BPRPEC water absorption, the linear models demonstrated favorable values for the P-value, R-squared, and adjusted R-squared, as illustrated in Table 16 and Figures 8(g) and 8(h). In Figures 8(g) and 8(h), the color gradient ranges from blue (indicate lowest), yellow (indicate medium), and magneta (indicate highest) water absorption. The Predicted R^2 of 0.8313 is reasonably consistent with the Adjusted R^2 of 0.9161, with a difference of less than 0.2. The signal-to-noise ratio was measured with sufficient precision, with a preferable ratio of more than four. In this case, the signal was adequate, with a ratio of 17.1328, allowing for effective navigation of the design space using this model. Similarly, Figure 9(d) illustrates that the actual and model-predicted results for each bamboo fiber content with different chopped glass fiber content exhibit good agreement with only minor differences, further emphasizing the model's enhanced predictive capabilities. The regression equation for water absorption (equations (15) and (17)) included only important components.

When we summarize the experimental and statistical results obtained for BFRPEC, the result obtained showed 5 wt. % of CGF has better mechanical and physical properties because the mixing of CFG within the matrix is very easy and the agglomeration is high in this case. So, at this point, the thermal stability of the maximum tensile, flexural, and impact was investigated compared to the unfilled one which is at BF8 and BF7 respectively.

Coded Regression Model

$$\text{Water Absorption (BFRPEC)} = 1.35 + 0.8437x_1 - 0.2330x_2 - 0.1155x_1x_2, \quad (14)$$

$$\text{Water Absorption (BPRPEC)} = 1.14 + 0.6917x_1 - 0.2633x_2. \quad (15)$$

Table 14: Water absorption result of BPRPEC with CGF filler content along with a replica of the test sample.

Sample	BPRPEC water absorption (%)				Standard deviation
	Specimen 1	Specimen 2	Specimen 3	Average	
BP1	0.614	0.613	0.627	0.618	0.0063
BP2	0.53	0.53	0.58	0.54	0.023
BP3	0.42	0.4	0.44	0.42	0.0163
BP4	1.53	1.66	1.58	1.59	0.053
BP5	1265	1.255	1.24	1.25	0.01027
BP6	1	1	1.15	1.05	0.07
BP7	2.65	2.45	2.7	2.6	0.108
BP8	2.08	2.13	2.09	2.1	0.0216
BP9	1.93	1.91	1.98	1.94	0.029

Table 15: ANOVA model summary for water absorption of BFRPEC with CGF filler.

Source	*P*-value	*R*-squared	Adjusted *R*-squared	Predicted *R*-squared	Adequate precision
Linear	0.0001	0.9806	0.9741	0.9447	30.2927
2FI	0.00001	0.9920	0.9753	0.8908	23.6219

Table 16: ANOVA Model summary for water absorption of BPRPEC with CGF filler.

Source	*P*-value	*R*-squared	Adjusted *R*-squared	Predicted *R*-squared	Adequate precision
Linear	0.00024	0.937	0.916	0.8313	17.13
Quadratic	0.00298	0.99	0.975	0.89	23.62

Actual Regression Model

$$\text{Water Absorption (BFRPEC)} = -3.8725 + 0.154000\,\text{BF wt\%} - 0.056000\,\text{CGF wt\%}, \quad (16)$$

$$\text{Water Absorption (BPRPEC)} = -3.44311 + 0.1384\text{BP wt\%} - 0.052667\,\text{CGF wt\%}. \quad (17)$$

In summary both BFRPEC and BPRPEC improved with CGF addition: Compared to unfilled composites, both composites showed increased tensile strength, flexural strength, and impact strength with CGF addition.

BFRPEC achieved higher values: The composite with BF8 had the highest tensile (131.22 MPa), flexural (128.76 MPa), and impact strength (113.3 kJ/m^2) compared to short fibers. BPRPEC had lower water absorption: The water absorption of BPRPEC composites was lower than BFRPEC composites, regardless of CGF content. CGF had minimal effect on BPRPEC water absorption:

3.9. Experimental Analysis of Thermogravimetric Analysis (TGA). The thermal stability of BFRPEC with CGF filler and without CGF was investigated with thermogravimetric analysis (TGA). Both composites showed a one-step degradation. For BFRPEC with CGF, the weight loss begins at 250°C and is due to the burning of the natural fiber components of the composites. The onset of degradation occurs at around 255°C. Approximately 80 and 70 percent of weight loss was observed for BF8 and BF7, respectively, at 250°C. For bamboo fiber-alone composites and filler-added composites, this weight loss occurred at 250 and 255°C, respectively as we observe in Figure 14.

3.10. Overall Statistical Analysis. The summary statistics of the models from Design-Expert version 13 software are shown in Tables 17 and 18, below. The best model is the one that has the highest *R*-squared, adjusted *R*-squared or predicted *R*-squared values that are close to unity and/or have close values [54]. The gap between the adjusted *R*-squared and *R*-squared values should not exceed 0.2 for an acceptable model. However, according to [55] a high *R*-squared value does not always reflect a good regression model, and such a conclusion can only be drawn based on a similarly high adjusted *R*-squared, implying that the model is appropriate for prediction across a variety of experimental variables [56]. Moreover, the difference between adjusted and predicted *R*-squared should be less than 0.2 to ensure model prediction beyond the experimental range [57]. Additional statistical measures in model validation are the adequate precision and *P*-values of the developed models. Adequate precision is a measure of acceptable signal-to-noise ratio where a value higher than 4 is acceptable. A *P*-value less than 0.05 indicates the statistical significance of the model (good in predicting the output response with a 5% chance that the model value could occur due to noise). Values greater than 0.1000 are indicated as statistically insignificant.

Table 17: Coded design points and experimental results for BFRPEC with CGF filler.

Run	Short name	Factors		Response			
		X_1, (A) (wt.%)	X_2, (B) (wt.%)	Tensile strength (MPa)	Flexural strength (MPa)	Impact strength (kJ/m^2)	Water absorption (%)
1	BF1	−1	−1	94.5	73.21	58.35	0.618
2	BF2	−1	0	126.93	98.4	79.6	0.54
3	BF3	−1	1	120.56	96.8	74.6	0.42
4	BF4	0	−1	105.3	80.35	70.5	1.59
5	BF5	0	0	129.58	111.46	107.8	1.25
6	BF6	0	1	125.71	104.44	98.8	1.05
7	BF7	1	−1	112.23	89.49	82.3	2.6
8	BF8	1	0	131.22	128.76	113.3	2.1
9	BF9	1	1	126.9	126.82	107.8	1.94

Table 18: Coded design points and experimental results for BPRPEC with CGF filler.

Run	Short name	Factors		Response			
		X_1, (A) (wt.%)	X_2, (B) (wt.%)	Tensile strength (MPa)	Flexural strength (MPa)	Impact strength (kJ/m^2)	Water absorption (%)
1	BP1	30	0	73.22	41.54	33.2	0.57
2	BP2	30	5	83.6	49.09	44.7	0.46
3	BP3	30	10	95	68.4	47.6	0.38
4	BP4	35	0	80.25	46.05	69.6	1.59
5	BP5	35	5	87.73	65.7	76.2	1.057
6	BP6	35	10	99.96	77.94	83	1.05
7	BP7	40	0	85	51.25	88.22	2.13
8	BP8	40	5	89.925	76.57	89.9	1.78
9	BP9	40	10	102	79.54	91.7	1.65

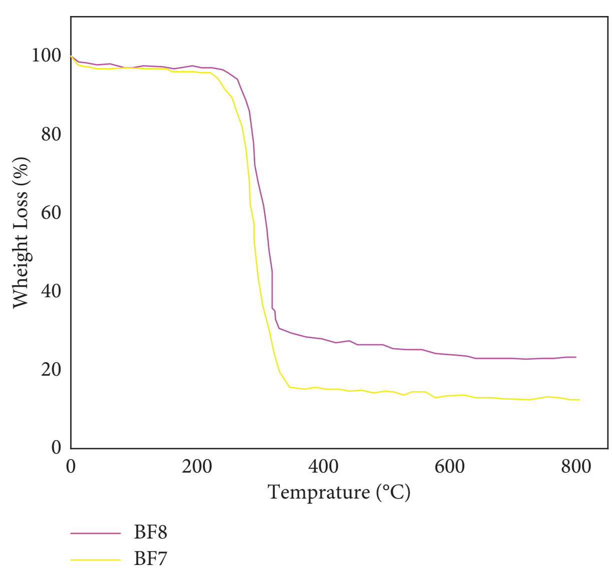

Figure 14: Thermogravimetric analysis of 40 wt.% BFRPEC with 0 and 5% weights of chopped glass fiber filler.

3.10.1. Different Models for BFRPEC and BPRPEC. The mechanical properties of BFRPEC fit a quadratic model, while BPRPEC fit a linear model. Water absorption followed a linear two-factor interaction model for BFRPEC and a linear model for BPRPEC. Impact energy followed a quadratic model for BPRPEC. The water absorption of BPRPEC composites showed a linear relationship with fiber content, and CGF addition had little impact. BFRPEC water absorption had complex interaction: The water absorption of BFRPEC composites showed a 2FI linear model with fiber content and CGF interaction, suggesting a more complex relationship.

3.10.2. Agreement between the Model and the Experiment. Overall, the statistical models accurately predicted the experimental results, suggesting their potential for future property prediction.

Table 19: ANOVA and significance of each parameter on tensile strength for BFRPEC with CGF filler.

Source	Sum of squares	Df	Mean-square	*F*-value	*P*-value	Significance
Quadratic model	1246.44	5	249.29	35.73	0.0071	Significant
A (BF wt.%)	134.05	1	134.05	19.21	0.0220	Significant
B (CGF wt.%)	623.02	1	623.02	89.29	0.0025	Significant
AB	32.43	1	32.43	4.65	0.1200	Insignificant
A^2	4.34	1	4.34	0.6222	0.4878	Significant
B^2	452.60	1	452.60	64.86	0.0040	Insignificant
Residual	20.93	3	6.98			
Cor total	1267.38	8				

Table 20: ANOVA and significance of each parameter on tensile strength for BPRPEC with CGF filler.

Source	Sum of squares	Df	Mean-square	*F*-value	*P*-value	Significance
Linear model	675.22	2	337.61	96.33	0.0001	Significant
X_1	105.04	1	105.04	26.97	0.0016	Significant
X_2	570.18	1	570.18	162.69	0.0001	Significant
Residual	21.03	6	3.50			
Core total	696.25	8				

(1) Tensile Strength. As shown in Tables 19 and 20, the model's *F*-value of 35.73 and 96.33 shows that it is significant for both long and short bamboo fiber respectively. An *F*-value this large could happen due to noise only 0.71 and 0.76 percent in the case of long and short bamboo respectively. Model variables are significant if the *P*-value is less than 0.0500 and also x_1, x_2, and ${x_2}^2$ are significant model variables in the case of long bamboo fiber as shown in equations (2) and (4). Values greater than 0.1000 show that the model variable is insignificant. But in the case of short bamboo fiber x_1 , and x_2 are significant model variables and the *P*-value is less than 0.0500 as shown in equations (3) and (5).

Where: x_1 or A: -is Long/short bamboo fiber weight (BF/BP wt%), x_2 or B: -is chopped glass fiber weight (CGF wt%)

(2) Flexural Strength. As shown in Tables 21 and 22 the model's *F*-value of 52.79 and 37.67 shows that it is significant for both long and short bamboo fiber respectively. An *F*-value this large could happen due to noise only 0.40 and 0.04% percent of the time in the case of long and short bamboo respectively. Model variables are significant if the *P*-value is less than 0.0500 and also x_1, x_2, and ${x_2}^2$ are significant model variables in the case of long bamboo fiber as shown in equations (6) and (8). But in the case of short bamboo fiber x_1 , and x_2 are significant model variables and the *P*-value is less than 0.0500 as shown in equations (7) and (9).

(3) Impact Strength. As shown in Tables 23 and 24, the model's *F*-values of 34.19 and 153.73 show that it is significant for both long and short bamboo fiber respectively. An *F*-value this large could happen due to noise only 0.76 and 0.08 percent of the time in the case of long and short bamboo respectively. Model terms are significant if the *P*-value is less than 0.0500. x_1 , x_2, and ${x_2}^2$ are significant model variables in both cases as shown in equations (10) and (12) for long bamboo fiber and also as shown in equations (11) and (13) for short bamboo fiber.

(4) Water Absorption. As shown in Tables 25 and 26, The model's *F*-values of 44.68 and 64.44 indicate that it is significant for both long and short bamboo fiber respectively. An *F*-value this large could happen due to noise only 0.02 and 0.01 percent of the time in the case of long and short bamboo respectively. Model variables are significant if the *P*-value is less than 0.0500. In this case, A and B are important model terms in both cases as shown in equations (14) and (16) for long bamboo fiber and also as shown in equations (15) and (17) for short bamboo fiber. Values higher than 0.1000 show that the model variable does not affect response.

Comparative Analysis of BFRPEC/BPRPEC with CGF Filler Mechanical Properties with those from previous published work.

The comparative analysis between different previous work was studied and presented in Table 27 below for different property based on the information obtained from [58, 59].

In a comparison to other studies like Reddy, et al. [62] which examined the tensile characteristics of glass to bamboo fiber-reinforced polyester hybrid composites. This study reported a tensile strength of 95 MPa, which was lower than the tensile strength obtained in this study. On other hand Rao et al. [63] also investigated the tensile characteristics of bamboo fiber filled with fly ash-reinforced composite at various volume fractions and obtained a tensile strength of 77.53 MPa, flexural strength of 113.35 MPa at 0.525. The obtained tensile strength was lower than the tensile strength resulting in this study, which was 102 MPa. Similarly, Vaghasia and Rachchh [64] investigated the mechanical properties of a bamboo glass polyester hybrid composite. They found that the tensile strength of their composite, with a comparable fiberglass content, was only 42 MPa, which is significantly lower than the 102 MPa obtained in the current study for the composite of 40 to 10 wt.% bamboo fibers to chopped fiberglass. Olorunnishola and Adubi [65] compared and evaluated Jute reinforced glass

Table 21: ANOVA and significance of each parameter on flexural strength for BFRPEC with CGF filler.

Source	Sum of squares	Df	Mean-square	F-value	P-value	Significance
Quadratic model	2881.31	5	576.26	52.79	0.0040	Significant
A-BF wt.%	979.46	1	979.46	89.72	0.0025	Significant
B-CGF wt.%	1204.45	1	1204.45	110.34	0.0018	Significant
AB	47.20	1	47.20	4.32	0.1291	Insignificant
A^2	24.45	1	24.45	2.24	0.2314	Insignificant
B^2	625.75	1	625.75	57.32	0.0048	Significant
Residual	32.75	3	10.92			
Cor total	2914.06	8				

Table 22: ANOVA and significance of each parameter on flexural strength for BPRPEC with CGF filler.

Source	Sum of squares	Df	Mean-square	F-value	P-value	Significance
Linear model	1651.96	2	825.98	37.67	0.0004	Significant
X_1	389.30	1	389.30	17.76	0.0056	Significant
X_2	1262.66	1	1262.66	57.59	0.0003	Significant
Residual	131.55	6	21.92			
Core total	1783.51	8				

Table 23: ANOVA and significance of each parameter on impact strength for BFRPEC with CGF filler.

Source	Sum of squares	Df	Mean-square	F-value	P-value	Significance
Quadratic model	2956.79	5	591.36	34.19	0.0076	Significant
A-BF wt.%	1375.62	1	1375.62	79.54	0.0030	Significant
B-CGF wt.%	817.83	1	817.83	47.29	0.0063	Significant
AB	21.39	1	21.39	1.24	0.3472	Insignificant
A^2	81.28	1	81.28	4.70	0.1187	Insignificant
B^2	660.66	1	660.66	38.20	0.0085	Significant
Residual	51.88	3	17.29			
Cor total	3008.67	8				

Table 24: ANOVA and significance of each parameter on impact strength for BPRPEC with CGF filler.

Source	Sum of squares	Df	Mean-square	F-value	P-value	Significance
Quadratic model	3883.56	5	776.71	153.73	0.0008	Significant
A-BF wt.%	3471.38	1	3471.38	687.06	0.0001	Significant
B-CGF wt.%	163.07	1	163.07	32.28	0.0108	Significant
AB	29.81	1	29.81	5.90	0.0073	Insignificant
A^2	215.49	1	215.49	42.95	0.4491	Insignificant
B^2	3.81	1	3.81	0.7538		
Residual	15.16	3	5.05			
Cor total	3898.72	8				

Table 25: ANOVA and significance of each parameter on water absorption for BFRPEC with CGF filler.

Source	Sum of squares	Df	Mean-square	F-value	P-value	Significance
2FI linear model	4.03	2	2.01	44.68	0.0002	Significant
A-BF wt.%	3.56	1	3.56	78.93	0.0001	Significant
B-CGF wt.%	0.4704	1	0.4704	10.44	0.0179	Significant
Residual	0.2704	6	0.0451			
Cor total	4.30	8				

fiber to polypropylene composites. The impact behavior of the material was assessed. By hand layup technique, samples of hybrid jute reinforced (PJG) (30 wt.% jute/10 wt.% glass), jute fiber-reinforced propylene PJ (40 wt.% jute), and glass fiber-reinforced propylene (PG) (40 wt.% glass) matrix. With Hybrid PJG, the impact strength is 11.61 J. In this case, the lowest impact energy obtained was 14 J or 33.2, which is higher than that of jute glass fiber-reinforced polypropylene.

Table 26: ANOVA and significance of each parameter on water absorption for BPRPEC with CGF filler.

Source	Sum of squares	Df	Mean-square	F-value	P-value	Significance
Linear model	3.29	2	1.64	64.44	0.00024	Significant
A-BF wt%	2.87	1	2.87	112.57	<0.0001	Significant
B-CGF wt%	0.4161	1	0.4161	16.32	0.0068	Significant
Residual	0.1530	6	0.0255			
Cor total	3.44	8				

Table 27: Comparison of properties of long and short bamboo fiber reinforced polyester with CGF composites with those from published work.

Properties	BFRPEC/BPRPEC with chopped glass fiber filler composites (current work)		Isophthalic polyester with Sandwich composites [48]		Graphite modified cotton fiber reinforced polyester composites [60]	Studies on tensile and compression characteristics of silk-cotton reinforced composite [61]
	BF8	BP9	C1	C2	CFRPE	SCRPE
Tensile strength (MPa)	131.22	102	30	42	38	63.15
Tensile modulus (GPa)	4.877	3.233	0.8	1.3	4.2	6.0
Flexural strength (MPa)	128.76	79.54	38	32	142	109.03
Flexural modulus (GPa)	4.16	2.95	2.3	1.9	—	—

Therefore, the results of the present study demonstrate a superior tensile strength for the composite, indicating the effectiveness of the bamboo fiber polyester hybridized with the chopped glass fiber approach.

4. Conclusions

The findings of this study have significant implications for the development and application of the composite material. The key findings and their potential applications are as follows:

(1) Enhanced Mechanical Properties: The composite material exhibited improved ultimate tensile strength, tensile modulus, flexural strength, and flexural modulus compared to the unfilled material. These enhancements indicate that the composite has increased resistance to tensile and bending forces, as well as improved stiffness. This makes the composite suitable for structural applications where high strength and rigidity are required.

(2) Improved Impact Resistance: The composite material demonstrated a significant increase in impact energy, indicating enhanced toughness and the ability to withstand impact forces. This makes the composite suitable for applications where impact resistance is crucial, such as automotive components, sporting goods, and protective equipment.

(3) Enhanced Thermal Stability: The composite material exhibited improved thermal stability, with a relatively high degradation temperature. This makes it suitable for applications in high-temperature environments, such as aerospace components, engine parts, and industrial equipment that are exposed to elevated temperatures.

(4) Mathematical Models: The study developed mathematical models to analyze the relationship between the factors (weight percentages of bamboo fiber and chopped glass fiber) and various responses. These models provide insights into the optimization of the composite material, allowing for the prediction and control of its mechanical and physical properties during the design and manufacturing processes.

(5) Significance of Parameters: The study identified the weight percentages of both long bamboo fiber and chopped glass fiber as significant parameters in determining the mechanical and thermal properties of the composite material. This knowledge enables targeted optimization of the composite by adjusting these parameters to achieve desired performance characteristics.

(6) Further Investigation: The study suggests that further investigation and characterization are needed to determine the exact mechanism responsible for performance differences between different filler compositions. This would enhance the understanding of the composite's behavior and guide future material design and optimization efforts.

(7) Variable Screening: Future studies are recommended to screen other variables that may affect the responses beyond the weight percentages of reinforcement and filler. This broader exploration can provide a more comprehensive understanding of the factors influencing the composite's performance and guide further improvements.

(8) Different Fabrication Methods: The impact of various fabrication methods on bamboo fiber-

reinforced polyester composites with milled glass fiber should be studied. This investigation would enable the selection of the most suitable fabrication technique for achieving the desired mechanical and physical properties.

(9) Recycling Methods for Filler Material: Further study should explore different waste glass fiber recycling methods for filler material in bamboo fiber-reinforced polymer composites. This research can contribute to sustainable manufacturing practices by utilizing recycled materials and reducing environmental impact.

(10) Future studies should consider increasing the sample size to strengthen the reliability of the findings.

In summary, the findings of this study demonstrate the enhanced mechanical properties, improved impact resistance, and thermal stability of the composite material. These outcomes open up opportunities for its application in diverse industries, including construction, automotive, aerospace, and sports. Further research is recommended to explore additional variables, fabrication methods, and recycling approaches to advance the field of bamboo fiber-reinforced composites.

Data Availability

The data used to support the findings of this study are included within the supplementary information file.

Conflicts of Interest

The authors declare that they have no known conflicts financial interests or personal relationships that could have appeared to influence the work reported in this manuscript.

Authors' Contributions

Mohammed Abdulkedir Alfeki (lecturer in the Department of Mechanical Engineering) contributed to the Conceptualization of the study, Methodology, Validation, Software, Resources, Investigation, Data Curation, Writing - Original Draft Preparation, Formal Analysis, Visualization, Supervision, Project Administration, and Funding Acquisition of the manuscript. Ephrem Assefa Feyissa (lecturer in the Department of Mechanical Engineering) contributed to the Writing - Review and editing of the manuscript.

Supplementary Materials

Figure S1: Water retting process of the bamboo strip. Figure S2: NaOH flakes for treatment of the bamboo fiber. Figure S3: (a) Treatment process and (b) treated fiber Figure S4: (a) waste glass fiber and (b) chopped or milled glass fiber. Figure S5: Milling cutter machine at Bahir Dar University. Figure S6: Universal testing machine for both flexural and tensile tests. Figure S7: Charpy impact testing machine. Figure S8: Tensile test specimen of (a) BFRPEC (b) BPRPEC with CGF filler. Figure S9: Flexural test specimen of (a) BFRPEC (b) BPRPEC with CGF filler. Figure S10: Impact test specimen of (a) BFRPEC (b) BPRPEC with CGF filler. Figure S11: Water absorption specimen of (a) BFRPEC (b) BPRPEC with CGF filler. Figure S12: Setup for thermogravimetric analysis BFRPEC with CGF filler. (*Supplementary Materials*)

References

[1] M. Bhong, T. K. Khan, K. Devade et al., "Review of composite materials and applications," *Materials Today: Proceedings*, 2023.

[2] M. Q. Zhang, M. Z. Rong, and X. Lu, "Fully biodegradable natural fiber composites from renewable resources: all-plant fiber composites," *Composites Science and Technology*, vol. 65, no. 15-16, pp. 2514–2525, 2005.

[3] D. B. Dittenber and H. V. GangaRao, "Critical review of recent publications on use of natural composites in infrastructure," *Composites Part A: Applied Science and Manufacturing*, vol. 43, no. 8, pp. 1419–1429, 2012.

[4] S. R. Mousavi, M. H. Zamani, S. Estaji et al., "Mechanical properties of bamboo fiber-reinforced polymer composites: a review of recent case studies," *Journal of Materials Science*, vol. 57, no. 5, pp. 3143–3167, 2022.

[5] A. Ali, K. Shaker, Y. Nawab et al., "Hydrophobic treatment of natural fibers and their composites—a review," *Journal of Industrial Textiles*, vol. 47, no. 8, pp. 2153–2183, 2018.

[6] A. Mohanty, M. Misra, and L. T. Drzal, "Surface modifications of natural fibers and performance of the resulting biocomposites: an overview," *Composite Interfaces*, vol. 8, no. 5, pp. 313–343, 2001.

[7] Z. Azwa and B. Yousif, "Physical and mechanical properties of bamboo fibre/polyester composites subjected to moisture and hygrothermal conditions," *Proceedings of the Institution of Mechanical Engineers, Part L: Journal of Materials: Design and Applications*, vol. 233, no. 6, pp. 1065–1079, 2019.

[8] C. Harito, D. V. Bavykin, B. Yuliarto, H. K. Dipojono, and F. C. Walsh, "Polymer nanocomposites having a high filler content: synthesis, structures, properties, and applications," *Nanoscale*, vol. 11, no. 11, pp. 4653–4682, 2019.

[9] N. Saba, P. Tahir, and M. Jawaid, "A review on potentiality of nano filler/natural fiber filled polymer hybrid composites," *Polymers*, vol. 6, no. 8, pp. 2247–2273, 2014.

[10] B. P. Chang, A. Gupta, R. Muthuraj, and T. H. Mekonnen, "Bioresourced fillers for rubber composite sustainability: current development and future opportunities," *Green Chemistry*, vol. 23, no. 15, pp. 5337–5378, 2021.

[11] K. Zhang, F. Wang, W. Liang, Z. Wang, Z. Duan, and B. Yang, "Thermal and mechanical properties of bamboo fiber reinforced epoxy composites," *Polymers*, vol. 10, no. 6, p. 608, 2018.

[12] R. Mateus, S. Neiva, L. Bragança, P. Mendonça, and M. Macieira, "Sustainability assessment of an innovative lightweight building technology for partition walls–comparison with conventional technologies," *Building and Environment*, vol. 67, pp. 147–159, 2013.

[13] F. S. Merritt, *Building Design and Construction Handbook*, McGraw-Hill, NY, USA, 2001.

[14] S. Ojha, H. Bisaria, S. Mohanty, and K. Kanny, "Mechanical performance of e-glass reinforced polyester resins (isophthalic and orthophthalic) laminate composites used in marine applications," *Proceedings of the Institution of Mechanical Engineers, Part L: Journal of Materials: Design and Applications*, vol. 24, 2023.

[15] B. Abu-Jdayil, A.-H. Mourad, W. Hittini, M. Hassan, and S. Hameedi, "Traditional, state-of-the-art and renewable thermal building insulation materials: an overview," *Construction and Building Materials*, vol. 214, pp. 709–735, 2019.

[16] H. S. Hens, *Performance Based Building Design 2: From Timber-Framed Construction to Partition Walls*, John Wiley & Sons, NJ, USA, 2012.

[17] J. L. Thomason, "Glass fibre sizing: a review," *Composites Part A: Applied Science and Manufacturing*, vol. 127, 2019.

[18] S. Devaraju and M. Alagar, "Unsaturated polyester—macrocomposites," in *Unsaturated Polyester Resins*, pp. 43–66, Elsevier, Amsterdam, The Netherlands, 2019.

[19] L. Silva, C. Angrizani, J. Souza, S. Amico, and J. Medeiros, "Use of polyester/glass-fiber residues as fillers for composites," *Journal of Applied Polymer Science*, vol. 124, no. 1, pp. 302–310, 2012.

[20] S. Sugiman, P. D. Setyawan, and B. Anshari, "Effect of fiber length on the mechanical properties and water absorption of bamboo fiber/polystyrene-modified unsaturated polyester composites," *IOP Conference Series: Materials Science and Engineering*, vol. 532, no. 1, 2019.

[21] S. A. A. Z. Mat Darus, M. J. Ghazali, C. H. Azhari, R. Zulkifli, and A. A. Shamsuri, "Mechanical properties of Gigantochloa scortechinii bamboo particle reinforced semirigid polyvinyl chloride composites," *Jurnal Teknologi*, vol. 82, no. 2, 2020.

[22] L. Jiang, Y. Li, C. Xiong, S. Su, and H. Ding, "Preparation and properties of bamboo fiber/nano-hydroxyapatite/poly(lactic-co-glycolic) composite scaffold for bone tissue engineering," *ACS Applied Materials and Interfaces*, vol. 9, no. 5, pp. 4890–4897, 2017.

[23] H. Bisaria, M. Gupta, P. Shandilya, and R. Srivastava, "Effect of fibre length on mechanical properties of randomly oriented short jute fibre reinforced epoxy composite," *Materials Today: Proceedings*, vol. 2, no. 4-5, pp. 1193–1199, 2015.

[24] F. S. da Luz, F. D. C. Garcia Filho, M. T. G. Del-Rio, L. F. C. Nascimento, W. A. Pinheiro, and S. N. Monteiro, "Graphene-incorporated natural fiber polymer composites: a first overview," *Polymers*, vol. 12, no. 7, p. 1601, 2020.

[25] S. Ojha, H. Bisaria, S. Mohanty, and K. Kanny, "Experimental investigation on mechanical performance of PVC foam-based E-glass isophthalic polyester composites," *Polymer Composites*, vol. 45, no. 2, pp. 1762–1775, 2024.

[26] W. Wang, M. Sain, and P. Cooper, "Study of moisture absorption in natural fiber plastic composites," *Composites Science and Technology*, vol. 66, no. 3-4, pp. 379–386, 2006.

[27] H. Chen, V. V. Ginzburg, J. Yang et al., "Thermal conductivity of polymer-based composites: fundamentals and applications," *Progress in Polymer Science*, vol. 59, pp. 41–85, 2016.

[28] N. Nurazzi, M. Asyraf, S. Fatimah Athiyah et al., "A review on mechanical performance of hybrid natural fiber polymer composites for structural applications," *Polymers*, vol. 13, no. 13, p. 2170, 2021.

[29] Z. Khan, B. Yousif, and M. Islam, "Fracture behaviour of bamboo fiber reinforced epoxy composites," *Composites Part B: Engineering*, vol. 116, pp. 186–199, 2017.

[30] F. Yang, H. Long, B. Xie et al., "Mechanical and biodegradation properties of bamboo fiber-reinforced starch/polypropylene biodegradable composites," *Journal of Applied Polymer Science*, vol. 137, no. 20, 2020.

[31] S. K. Chattopadhyay, R. Khandal, R. Uppaluri, and A. K. Ghoshal, "Bamboo fiber reinforced polypropylene composites and their mechanical, thermal, and morphological properties," *Journal of Applied Polymer Science*, vol. 119, no. 3, pp. 1619–1626, 2011.

[32] T.-C. Yang, T.-L. Wu, K.-C. Hung, Y.-L. Chen, and J.-H. Wu, "Mechanical properties and extended creep behavior of bamboo fiber reinforced recycled poly (lactic acid) composites using the time–temperature superposition principle," *Construction and Building Materials*, vol. 93, pp. 558–563, 2015.

[33] Y. Yu, H. Wang, F. Lu, G. Tian, and J. Lin, "Bamboo fibers for composite applications: a mechanical and morphological investigation," *Journal of Materials Science*, vol. 49, no. 6, pp. 2559–2566, 2014.

[34] D. Redda and A. Alene, "Experimental analysis of bamboo and e-glass fiber reinforced epoxy hybrid composite," *Journal of Materials Science and Engineering B*, vol. 6, no. 3, pp. 153–160, 2016.

[35] L. A. Pothan, Z. Oommen, and S. Thomas, "Dynamic mechanical analysis of banana fiber reinforced polyester composites," *Composites Science and Technology*, vol. 63, no. 2, pp. 283–293, 2003.

[36] A. I. Khuri and S. Mukhopadhyay, "Response surface methodology," *WIREs Computational Statistics*, vol. 2, no. 2, pp. 128–149, 2010.

[37] Q. Viel, A. Esposito, J.-M. Saiter, C. Santulli, and J. A. Turner, "Interfacial characterization by pull-out test of bamboo fibers embedded in poly (lactic acid)," *Fibers*, vol. 6, no. 1, p. 7, 2018.

[38] M. Cai, H. Takagi, A. N. Nakagaito, Y. Li, and G. I. Waterhouse, "Effect of alkali treatment on interfacial bonding in abaca fiber-reinforced composites," *Composites Part A: Applied Science and Manufacturing*, vol. 90, pp. 589–597, 2016.

[39] M. Mun'aim Idrus, A. M. Saat, M. M. Bazin, and R. Zoolfakar, "Fire retardant and physical properties of kapok-chopped strand mats fiberglass composites for marine application," in *Advancement in Emerging Technologies and Engineering Applications*, pp. 231–238, Springer, Cham, 2020.

[40] G. Liu, "A step-by-step method of rule-of-mixture of fiber-and particle-reinforced composite materials," *Composite Structures*, vol. 40, no. 3-4, pp. 313–322, 1997.

[41] N. Shanmugasundaram, I. Rajendran, and T. Ramkumar, "Static, dynamic mechanical and thermal properties of untreated and alkali treated mulberry fiber reinforced polyester composites," *Polymer Composites*, vol. 39, no. S3, pp. E1908–E1919, 2018.

[42] A. International, "ASTM D3039/D3039M-17, standard test method for tensile properties of polymer matrix composite materials," *Standard Test Method for Tensile Properties of Polymer Matrix Composite Materials*, 2017.

[43] A. International, *Standard Test Method for Flexural Properties of Polymer Matrix Composite Materials*, ASTM International, PY, USA, 2007.

[44] A. International, *Standard Test Method for Determining the Charpy Impact Resistance of Notched Specimens of Plastics. ASTM D6110-10*, ASTM International West Conshohocken, Pennsylvania, PY, USA, 2010.

[45] A. C. D. O. P. S. D. O. P. Properties, *Standard Test Method for Water Absorption of Plastics*, American Society for Testing and Materials, Pennsylvania, PY, USA, 1995.

[46] C. Nagaraj, D. Mishra, and J. Durga Prasad Reddy, "Estimation of tensile properties of fabricated multi layered natural jute fiber reinforced E-glass composite material," *Materials Today Proceedings*, vol. 27, pp. 1443–1448, 2020.

[47] A. N. Benítez, M. D. Monzón, I. Angulo, Z. Ortega, P. M. Hernández, and M. D. Marrero, "Treatment of banana fiber for use in the reinforcement of polymeric matrices," *Measurement*, vol. 46, no. 3, pp. 1065–1073, 2013.

[48] S. Ojha, H. Bisaria, S. Mohanty, and K. Kanny, “Fabrication and characterization of light weight PVC foam based E-glass reinforced polyester sandwich composites,” *Proceedings of the Institution of Mechanical Engineers-Part C: Journal of Mechanical Engineering Science*, vol. 237, no. 21, pp. 5042–5051, 2023.

[49] H. A. Sallal, “Effect of the addition coconut shell powder on properties of polyurethane matrix composite,” *Al-Nahrain Journal for Engineering Sciences*, vol. 17, no. 2, pp. 203–210, 2014.

[50] A. A. Adediran, A. A. Akinwande, O. A. Balogun, O. Olasoju, and O. S. Adesina, “Experimental evaluation of bamboo fiber/particulate coconut shell hybrid PVC composite,” *Scientific Reports*, vol. 11, no. 1, pp. 5465–5514, 2021.

[51] E. Muñoz and J. A. García-Manrique, “Water absorption behaviour and its effect on the mechanical properties of flax fibre reinforced bioepoxy composites,” *International journal of polymer science*, vol. 2015, pp. 1–10, 2015.

[52] P. Ramadevi, D. Sampathkumar, C. V. Srinivasa, and B. Bennehalli, “Effect of alkali treatment on water absorption of single cellulosic abaca fiber,” *Bioresources*, vol. 7, no. 3, pp. 3515–3524, 2012.

[53] Z. Mohd Nazarudin, J. Mohd Ariff, M. A. Kassim et al., “The effect of alkaline treatment on water absorption and tensile properties of non-woven kenaf polyester composite,” *Advanced Materials Research*, vol. 812, pp. 258–262, 2013.

[54] R. Fatoni: Product design of wheat straw polypropylene composite, 2012. http://hdl.handle.net/10012/6790.

[55] A. Koocheki, A. R. Taherian, S. M. Razavi, and A. Bostan, “Response surface methodology for optimization of extraction yield, viscosity, hue and emulsion stability of mucilage extracted from Lepidium perfoliatum seeds,” *Food Hydrocolloids*, vol. 23, no. 8, pp. 2369–2379, 2009.

[56] J. Müssig and N. Graupner, “Test methods for fibre/matrix adhesion in cellulose fibre-reinforced thermoplastic composite materials: a critical review,” *Reviews of Adhesion and Adhesives*, vol. 8, no. 2, pp. 68–129, 2020.

[57] H. Le Man, S. Behera, and H. Park, “Optimization of operational parameters for ethanol production from Korean food waste leachate,” *International journal of Environmental Science and Technology*, vol. 7, no. 1, pp. 157–164, 2010.

[58] B. Wankhede, H. Bisaria, S. Ojha, and V. S. Dakre, “A review on cotton fibre-reinforced polymer composites and their applications,” *Proceedings of the Institution of Mechanical Engineers, Part L: Journal of Materials: Design and Applications*, vol. 237, no. 6, pp. 1347–1362, 2023.

[59] S. Ojha, H. Bisaria, S. Mohanty, and K. Kanny, “Static and dynamic mechanical analyses of E-glass–polyester composite used in mass transit system,” *Emerging Materials Research*, vol. 12, no. 1, pp. 28–36, 2023.

[60] S. Hashmi, U. Dwivedi, and N. Chand, “Graphite modified cotton fibre reinforced polyester composites under sliding wear conditions,” *Wear*, vol. 262, no. 11-12, pp. 1426–1432, 2007.

[61] R. Manjunatha and Sangeevmurthy, “Studies on tensile and compression characteristics of silk-cotton reinforced composites,” *International Journal of Engineering Research*, vol. 8, pp. 331–336, 2019.

[62] E. Venkata Subba Reddy, A. Varada Rajulu, K. Hemachandra Reddy, and G. Ramachandra Reddy, “Chemical resistance and tensile properties of glass and bamboo fibers reinforced polyester hybrid composites,” *Journal of Reinforced Plastics and Composites*, vol. 29, no. 14, pp. 2119–2123, 2010.

[63] T. V. Rao, K. Venkatarao, and L. Ch, “Mechanical properties of bamboo fibre filled with fly ash filler R einforced hybrid C omposites,” *International Journal of Engineering Research and Technology*, vol. 3, no. 9, pp. 725–732, 2014.

[64] B. Vaghasia and N. Rachchh, “Evaluation of physical and mechanical properties of woven bamboo glass polyester hybrid composite material,” *Materials Today: Proceedings*, vol. 5, no. 2, pp. 7930–7936, 2018.

[65] A. A. G. Olorunnishola and E. G. Adubi, “A comparative analysis of a blend of natural jute and glass fibers with synthetic glass FibersComposites as car bumper materials,” *IOSR Journal of Mechanical and Civil Engineering (IOSR-JMCE) e-ISSN*, vol. 15, no. 3, pp. 67–71, 2018.